mass of 8 or 9 (444) minus a glutamic acid fragment (130). ^{13}C NMR (D_2O) data was as follows: δ 30.474 (C-8'), 31.394 (C-5), 35.131 (C-b), 35.487 (C-c), 44.254 and 44.314 (C-d), 64.954 (C-a), 65.638 and 65.940 (C-4), 68.660 and 69.106 (C-2), 105.180 and 105.276 (C-6'), 110.394 and 110.440 (C-3'), 114.743 (C-4'), 115.639 (C-7'), 128.479 and 128.571 (C-2'), 129.686 (C-3a'), 134.087 and 134.124 (C-1a'), 151.666 (C-5'), 170.667 (C=0), 175.841 (C=0), 180.444 (C=0), 181.246 (C=0). Thus, a total of 20 carbon resonances were observed in accord with the proposed structure of 8/9. However, several resonances appeared as closely-spaced double peaks of equal intensity indicative of an equimolar mixture of 8 and 9. The $^1H,^1H$-COSY NMR spectrum also clearly showed two sets of signals of equal intensity. For reasons discussed earlier, it has been tentatively concluded that in 8 the C(2)-H and C(4)-H protons are cis whereas in 9 they are trans.

(2*R*,4*R*)-α-Amino-4-[[(carboxymethyl)amino]carbonyl]-2-[(5-hydroxy-1*H*-indol-3-yl)methyl]-δ-oxo-3-thiazolidinepentanoic acid (8): ^1H NMR (D_2O) δ 7.376 (d, $J_{6',7'}$ = 8.4 Hz, 1 H, C(7')-H), 7.325 (s, 1 H, C(2')-H), 7.109 (d, $J_{4',6'}$ = 2.4 Hz, 1 H, C(4')-H), 6.834 (dd, $J_{4',6'}$ = 2.4 Hz, $J_{6',7'}$ = 8.4 Hz, 1 H, C(6')-H), 5.251 (dd, J = 5.7, 9.0 Hz, 1 H, C(2)-H), 4.820 (t, J = 7.5 Hz, 1 H, C(4)-H), 4.027 (t, J = 8.1 Hz, 1 H, C(a)-H), 3.997 (s, 2 H, C(d)-H_2), 3.836-3.781 (m, 2 H, C(c)-H_2), 3.763-3.630 (m, 2 H, C(b)-H_2), 3.513, 3.497 (dd, J = 5.7, 9.9 Hz, 1 H, and dd, J = 4.2, 9.9 Hz, 1 H, C(8')-H_2), 3.380, 3.304 (dd, J = 6.0, 12.3 Hz, 1 H, and dd, J = 7.5, 12.3 Hz, 1 H, C(5)-H_2).

(2*S*,4*R*)-α-Amino-4-[[(carboxymethyl)amino]carbonyl]-2-[(5-hydroxy-1*H*-indol-3-yl)methyl]-δ-oxo-3-thiazolidinepentanoic acid (9): ^1H NMR (D_2O) δ 7.376 (d, $J_{6',7'}$ = 8.4 Hz, 1 H, C(7')-H), 7.309 (s, 1 H, C(2')-H), 7.089 (d, $J_{4',6'}$ = 2.4 Hz, 1 H, C(4')-H), 6.834 (dd, $J_{4',6'}$ = 2.4 Hz, $J_{6',7'}$ = 8.4 Hz, 1 H, C(6')-H), 5.181 (t, J = 7.2 Hz, 1 H, C(2)-H), 4.685 (t, J = 7.8 Hz, 1 H, C(4)-H), 4.027 (t, J = 8.1 Hz, 1 H, C(a)-H), 3.997 (s, 2 H, C(d)-H_2), 3.836-3.781 (m, 2 H, C(c)-H_2), 3.763-3.630 (m, 2 H, C(b)-H_2), 3.548, 3.544 (dd, J = 5.7, 18.9 Hz, 1 H and dd, J = 8.1, 18.9 Hz, 1 H, C(8')-H_2), 3.409, 3.330 (dd, J = 7.5, 12.6 Hz, 1 H, and dd, J = 5.4, 12.6 Hz, 1 H, C(5)-H_2).

Acknowledgment. This work was supported by NIH Grant No. GM-32367. Additional support was provided by the Research Council and Vice Provost for Research Administration at the University of Oklahoma.

Supplementary Material Available: Delayed COSY ^1H NMR spectrum of the mixture of epimers 6 and 7 (1 page). Ordering information is given on any current masthead page.

Inhibitors of Blood Platelet cAMP Phosphodiesterase. 2. Structure-Activity Relationships Associated with 1,3-Dihydro-2*H*-imidazo[4,5-*b*]quinolin-2-ones Substituted with Functionalized Side Chains[1,2]

Nicholas A. Meanwell,* Bradley C. Pearce, Herbert R. Roth, Edward C. R. Smith, Donald L. Wedding, J. J. Kim Wright, John O. Buchanan,† Urzula M. Baryla,† Marianne Gamberdella,† Elizabeth Gillespie,† Donald C. Hayes,† Steven M. Seiler,† Hugh C. Stanton,† George B. Zavoico,† and J. Stuart Fleming†

Departments of Chemistry and Cardiovascular Biochemistry and Pharmacology, The Bristol-Myers Squibb Pharmaceutical Research Institute, 5 Research Parkway, Wallingford, Connecticut 06492. *Received February 7, 1992*

A series of 1,3-dihydro-2*H*-imidazo[4,5-*b*]quinolin-2-one derivatives, substituted at the 7-position with functionalized side chains, was synthesized and evaluated as inhibitors of human blood platelet cAMP phosphodiesterase (PDE) as well as ADP- and collagen-induced platelet aggregation, in vitro. Structural modifications focused on variation of the side-chain terminus, side-chain length, and side-chain connecting atom. Functionality incorporated at the side-chain terminus included carboxylic acid, ester and amide, alcohol, acetate, nitrile, tetrazole, and phenyl sulfone moieties. cAMP PDE inhibitory potency varied and was dependent upon the side-chain terminus and its relationship with the heterocyclic nucleus. Methylation at N-1 or N-3 of the heterocycle diminished cAMP PDE inhibitory potency. Several representatives of this structural class demonstrated potent inhibition of ADP- and collagen-induced blood platelet aggregation and were half-maximally effective at low nanomolar concentrations. Amides **13d**, **13f**, **13h**, **13k**, **13m**, and **13w** are substantially more potent than relatively simply substituted compounds. However, platelet inhibitory properties did not always correlate with cAMP PDE inhibition across the series, probably due to variations in membrane permeability. Several compounds inhibited platelet aggregation measured ex vivo following oral administration to rats. Ester **11b**, acid **12b**, amide **13d**, and sulfone **29c** protected against thrombus formation in two different animal models following oral dosing and were found to be superior to anagrelide (2) and BMY 20844 (5). However, ester **11b** and acid **12b** demonstrated a unique pharmacological profile since they did not significantly affect hemodynamic parameters in dogs at doses 100-fold higher than that required for complete prevention of experimentally induced vessel occlusion in a dog model of thrombosis.

Introduction

Clinical trials with inhibitors of blood platelet aggregation have established therapeutic benefit in a number of pathological conditions that have a thrombotic or thromboembolic component.[3-13] However, these studies have also revealed deficiencies associated with currently available drugs which offer the clinician imprecise and limited control over platelet function and are characterized by a high incidence of side effects.[5,14] Inhibitors of blood platelet cAMP phosphodiesterase (PDE) have been shown to prevent platelet aggregation in response to most physiologically-relevant stimuli (i.e. they demonstrate broad-spectrum activity) and have been explored both

† Department of Cardiovascular Biochemistry and Pharmacology.

(1) Presented in part at the 197th National Meeting of the American Chemical Society, Dallas, TX, April 9-14, 1989: (a) Meanwell, N. A. Inhibitors of Platelet cAMP Phosphodiesterase as Potential Anti-thrombotic Agents; MEDI 3. (b) Pearce, B. C.; Wedding, D. L.; Meanwell, N. A.; Wright, J. J. K.; Fleming, J. S.; Gillespie, E. Synthesis and Biological Evaluation of 7-Carbon Substituted 1,3-Dihydro-2*H*-imidazo-[4,5-*b*]quinolin-2-ones; MEDI 9.

(2) For part 1, see: Meanwell, N. A.; Roth, H. R.; Smith, E. C. R.; Wedding, D. L.; Wright, J. J. K.; Fleming, J. S.; Gillespie, E. 1,3-Dihydro-2*H*-imidazo[4,5-*b*]quinolin-2-ones—Inhibitors of Blood Platelet cAMP Phosphodiesterase and Induced Aggregation. *J. Med. Chem.* **1991**, *34*, 2906-2916.

0022-2623/92/1835-2672$03.00/0

Chart I

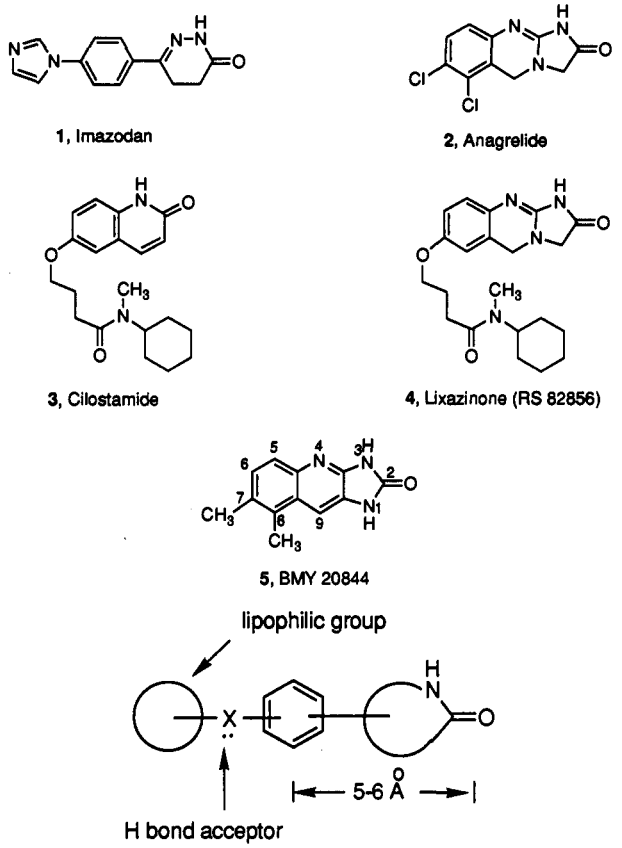

Figure 1. Structural elements common to low-K_m cAMP PDE inhibitors.

preclinically and clinically as antithrombotic agents.[15,16] The low-K_m, cGMP-inhibited cAMP PDE in platelets[17] that is the target of these agents appears to be nearly identical to a myocardial enzyme that regulates contractility.[18] Inhibitors of the heart enzyme, which also exhibit hypotensive properties as a consequence of inhibition of a vascular smooth muscle cAMP PDE,[19] have been the subject of extensive study over the last decade in an attempt to identify safe and effective replacements for the cardiac glycosides as agents for the treatment of congestive heart failure.[20,21] Computer-based molecular modeling studies of inhibitors of the cardiac isozyme have defined the pharmacophoric elements and equated them with structural features of the substrate cAMP.[22] The inhibitors of low-K_m cAMP PDE that have been employed to develop this model can be categorized into nonfused compounds, as exemplified by imazodan (1),[23] and the fused heterocyclics represented by anagrelide (2).[24] The im-

(3) Fuster, V.; Badimon, L.; Adams, P. C.; Turitto, V.; Cheseboro, J. Drugs Interfering with Platelet Functions: Mechanisms and Clinical Relevance. *Thrombosis and Haemostasis*; Verstraete, M., Vermylen, J., Lijnen, H. R., Arnout, J., Eds.; International Society on Thrombosis and Haemostasis and Leuven University Press: Leuven, 1987; pp 349–418.
(4) Gallus, A. S. The Use of Antithrombotic Drugs in Artery Disease. *Clin. Hematol.* **1986**, *15*, 509–559.
(5) Harker, L. A. Antiplatelet Drugs in the Management of Patients with Thrombotic Disorders. *Semin. Thromb. Hemostasis* **1986**, *12*, 134–155.
(6) Steering Committee of the Physicians' Health Study Research Group. Final Report on the Aspirin Component of the Ongoing Physicians' Health Study. *N. Engl. J. Med.* **1989**, *321*, 129–135.
(7) Stroke Prevention in Atrial Fibrillation Investigators. Stroke Prevention in Atrial Fibrillation Study, Final Results. *Circulation* **1991**, *84*, 527–539.
(8) Antiplatelet Trialists' Collaboration. Secondary Prevention of Vascular Disease by Prolonged Antiplatelet Treatment. *Br. Med. J.* **1988**, *296*, 320–331.
(9) Gent, M.; Blakely, J. A.; Easton, J. D.; Ellis, D. J.; Hachinski, V. C.; Harbison, J. W.; Panak, E.; Roberts, R. S.; Sicuirella, J.; Turpie, A. G. G. and the CATS Group. The Canadian American Ticlopidine Study (CATS) in Thromboembolic Stroke. *Lancet* **1989**, *1*, 1215–1220.
(10) Haas, W. K.; Easton, J. D.; Adams, H. P., Jr.; Pryse-Phillips, W.; Molony, B. A.; Anderson, S.; Kamm, B. A Randomized Trial Comparing Ticlopidine Hydrochloride with Aspirin for the Prevention of Stroke in High-Risk Patients. *N. Engl. J. Med.* **1989**, *321*, 501–507.
(11) Balsano, F.; Rizzon, P.; Violi, F.; Scrutinio, D.; Cimminiello, C.; Aguglia, F.; Pasotti, C.; Rudelli, G. and the Studio della Ticlopidina nell'Angina Instabile Group. Antiplatelet Treatment with Ticlopidine in Unstable Angina. *Circulation* **1990**, *82*, 17–26.
(12) Silver, M. J.; DiMinno, G. Aspirin as an Antithrombotic Agent. *Prog. Drug Res.* **1989**, *33*, 43–62.
(13) Giansante, G.; Calabrese, S.; Fisciaro, M.; Fiotti, N.; Mitri, E. Treatment of Intermittent Claudication with Antiplatelet Agents. *J. Int. Med. Res.* **1990**, *18*, 400–407.
(14) Harker, L. A.; Fuster, V. Pharmacology of Platelet Inhibitors. *J. Am. Coll. Cardiol.* **1986**, *8*, 21B–32B.
(15) Meanwell, N. A.; Seiler, S. M. Inhibitors of Platelet cAMP Phosphodiesterase. *Drugs Future* **1990**, *15*, 369–390.
(16) Meanwell, N. A.; Seiler, S. M. Platelet Activation and Drugs that Modify Platelet Function. *Drugs and the Delivery of Oxygen to Tissues*; Fleming, J. S., Ed.; CRC Press Inc.: Boca Raton, 1989; Chapter 5.
(17) Macphee, C. H.; Harrison, S. A.; Beavo, J. A. Immunological Identification of the Major Platelet Low-Km cAMP Phosphodiesterase: Probable Target for Anti-thrombotic Agents. *Proc. Natl. Acad. Sci. U.S.A.* **1986**, *83*, 6660–6663.
(18) Harrison, S. A.; Reifsnyder, D. H.; Gallis, B.; Cadd, G. G.; Beavo, J. A. Isolation and Characterization of Bovine Cardiac Muscle cGMP-Inhibited Phosphodiesterase: A Receptor for New Cardiotonic Drugs. *Mol. Pharmacol.* **1986**, *29*, 506–514.
(19) Lindgren, S.; Rascon, A.; Andersson, K-E.; Manganiello, V.; Degerman, E. Selective Inhibition of cGMP-Inhibited and cGMP-Noninhibited Cyclic Nucleotide Phosphodiesterases and Relaxation of Rat Aorta. *Biochem. Pharmacol.* **1991**, *42*, 545–552.
(20) Weishaar, R. E.; Cain, M. H.; Bristol, J. A. A New Generation of Phosphodiesterase Inhibitors: Multiple Molecular Forms of Phosphodiesterase and the Potential for Drug Selectivity. *J. Med. Chem.* **1985**, *28*, 537–545.
(21) Erhardt, P. W. In Search of the Digitalis Replacement. *J. Med. Chem.* **1987**, *30*, 231–237.
(22) (a) Rakhit, S.; Marciniak, G.; Leclerc, G.; Schwarz, J. Computer Assisted Pharmacophore Search in a Series of Nonsteroidal Cardiotonics. *Eur. J. Med. Chem.* **1986**, *21*, 511–515. (b) Davis, A.; Warrington, B. H.; Vinter, J. G. Strategic Approaches to Drug Design. II. Modelling Studies on Phosphodiesterase Substrates and Inhibitors. *J. Comput. Aided Mol. Des.* **1987**, *1*, 97–120. (c) Moos, W. H.; Humblet, C. C.; Sircar, I.; Rithner, C.; Weishaar, R. E.; Bristol, J. A.; McPhail, A. T. Cardiotonic Agents. 8. Selective Inhibitors of Adenosine 3′,5′-Cyclic Phosphate Phosphodiesterase III. Elaboration of a Five Point Model for Positive Inotropic Activity. *J. Med. Chem.* **1987**, *30*, 1963–1972. (d) Erhardt, P. W.; Hagedorn, A. A., III; Sabio, M. Cardiotonic Agents. 3. A Topographical Model of the Cardiac cAMP Phosphodiesterase Receptor. *Mol. Pharmacol.* **1988**, *33*, 1–13. (e) Erhardt, P. W.; Chou, Y-L. A Topographical Model for the cAMP Phosphodiesterase III Active Site. *Life Sci.* **1991**, *49*, 553–568.
(23) Sircar, I.; Duell, B. L.; Bobowski, G.; Bristol, J. A.; Evans, D. B. Cardiotonic Agents. 2. Synthesis and Structure–Activity Relationships of 4,5-Dihydro-6-[4-(1*H*-imidazo-1-yl)phenyl]-3-(2*H*)-pyridazinones: A New Class of Positive Inotropic Agents. *J. Med. Chem.* **1985**, *28*, 1405–1413.

Scheme I

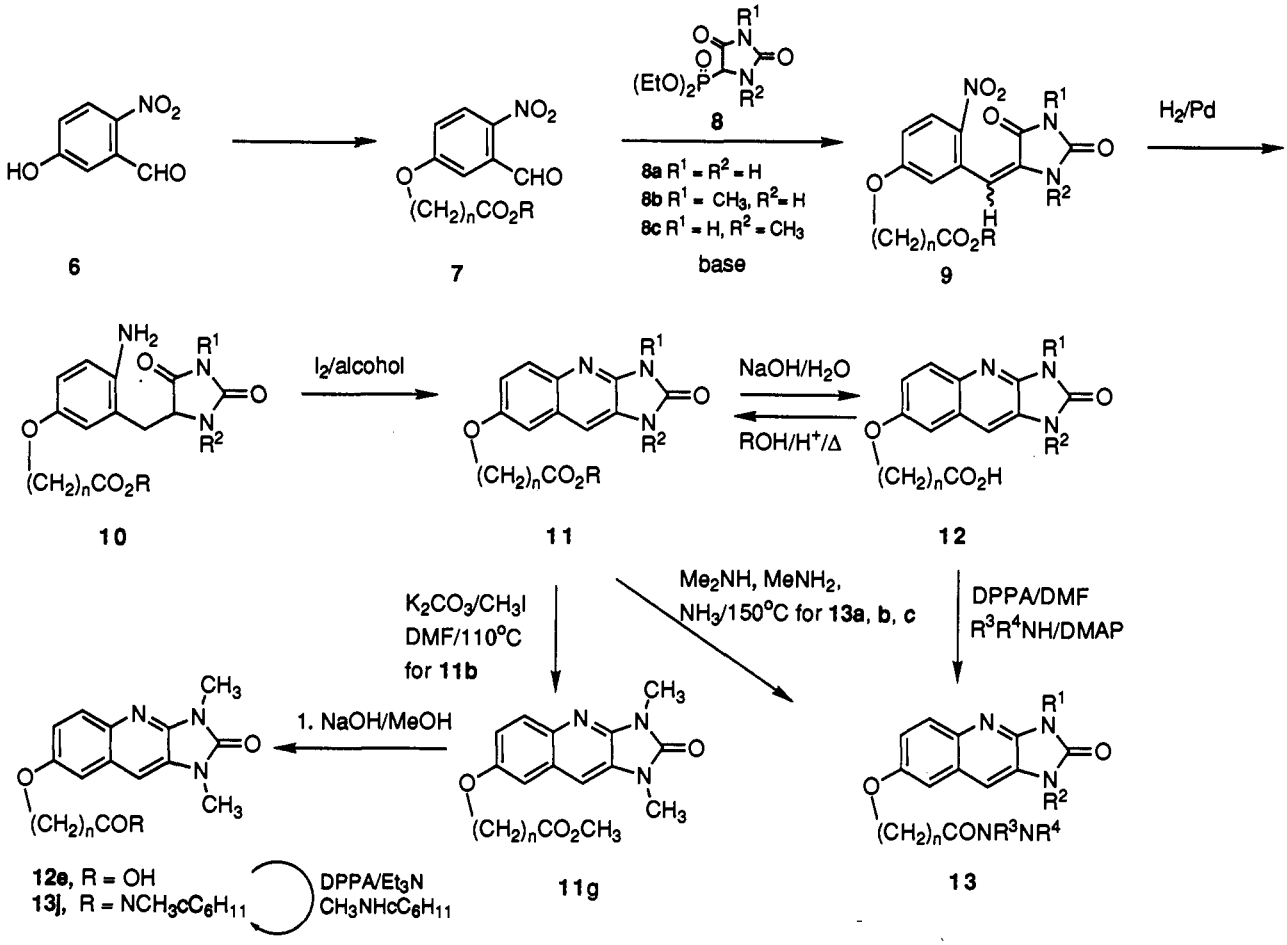

portant structural features, summarized in Figure 1, are postulated to interact with the catalytic domain of the enzyme and the pocket occupied by the adenine moiety of cAMP. Although these modeling studies have focused on interactions at the active site of the enzyme and its immediate vicinity, there exists a secondary binding site, remote from the catalytic center, that was originally identified with the discovery of cilostamide (**3**).[25] cAMP PDE inhibitors incorporating functionality able to take advantage of this interaction generally exhibit enhanced potency. This was most effectively demonstrated with the synthesis and biological evaluation of lixazinone (RS 82856) (**4**) which hybridizes structural elements of **2** and **3** into a molecule more potent than either progenitor.[26,27] However, there have been few attempts beyond these studies[25-27] to exploit this secondary binding region and successful application has been confined to the fused heterocyclic class of low-K_m cAMP PDE inhibitors.[28] We have recently demonstrated that 1,3-dihydro-2*H*-imidazo[4,5-*b*]quinolin-2-one derivatives are potent and selective inhibitors of blood platelet cAMP PDE that exhibit broad-spectrum inhibition of platelet aggregation in vitro.[2] BMY 20844 (**5**) was identified from this initial study as a clinical candidate on the basis of its pharmacological profile and efficacy in animal models of thrombosis.[29] As part of our effort to identify clinically useful

(24) (a) Tang, S. S.; Frojmovic, M. M. Inhibition of Platelet Function by Antithrombotic Agents which Selectively Inhibit Low K_m cyclic 3′,5′-adenosine monophosphate Phosphodiesterase. *J. Lab. Clin. Med.* **1980**, *95*, 241–257. (b) Gillespie, E. Anagrelide: A Potent and Selective Inhibitor of Platelet Cyclic AMP Phosphodiesterase Enzyme Activity. *Biochem. Pharmacol.* **1988**, *37*, 2866–2868. (c) Seiler, S. M.; Arnold, A. J.; Grove, R. I.; Fifer, C. A.; Keely, S. L., Jr.; Stanton, H. C. Effects of Anagrelide on Platelet cAMP Levels, cAMP-Dependent Protein Kinase and Thrombin-Induced Ca^{++} Fluxes. *J. Pharmacol. Exp. Ther.* **1987**, *243*, 767–774.

(25) (a) Nishi, T.; Yamamoto, K.; Shimizu, T.; Kanbe, T.; Kimura, Y.; Nakagawa, K. Studies on 2-Oxoquinoline Derivatives as Blood Platelet Aggregation Inhibitors. I. Alkyl 4-(2-Oxo-1,2,3,4-tetrahydro-6-quinolinyloxy)butyrates and Related Compounds. *Chem. Pharm. Bull.* **1983**, *31*, 798–810. (b) Nishi, T.; Tabusa, F.; Tanaka, T.; Shimizu, T.; Kanbe, T.; Kimura, Y.; Nakagawa, K. Studies on 2-Oxoquinoline Derivatives as Blood Platelet Aggregation Inhibitors. II. 6-[3-(1-Cyclohexyl-5-tetrazolyl)propoxy]-1,2-dihydro-2-oxoquinoline and Related Compounds. *Chem. Pharm. Bull.* **1983**, *31*, 1151–1157. (c) Nishi, T.; Tabusa, F.; Tanaka, T.; Ueda, H.; Shimizu, T.; Kanbe, T.; Kimura, Y.; Nakagawa, K. Studies on 2-Oxoquinoline Derivatives as Blood Platelet Aggregation Inhibitors. III. *N*-Cyclohexyl-*N*-(2-hydroxyethyl)-4-(1,2-dihydro-2-oxo-6-quinolinyloxy)butyramide and Related Compounds. *Chem. Pharm. Bull.* **1983**, *31*, 852–860.

(26) Jones, G. H.; Venuti, M. C.; Alvarez, R.; Bruno, J. J.; Berks, A. H.; Prince, A. Inhibitors of Cyclic AMP Phosphodiesterase. 1. Analogues of Cilostamide and Anagrelide. *J. Med. Chem.* **1987**, *30*, 295–303.

(27) Venuti, M. C.; Jones, G. H.; Alvarez, R.; Bruno, J. J. Inhibitors of Cyclic AMP Phosphodiesterase. 2. Structural Variations of *N*-cyclohexyl-*N*-methyl-4[(1,2,3,5-tetrahydro-2-oxoimidazo-[2,1-*b*]quinazolin-7-yl)oxy]butyramide (RS 82856). *J. Med. Chem.* **1987**, *30*, 303–318.

(28) (a) Lugnier, C.; Bruch, M.; Stoclet, J.-C.; Strub, M.-P.; Marivet, M.; Wermuth, C. G. Substituted Carbostyrils as Inhibitors of Cyclic AMP Phosphodiesterase. *Eur. J. Med.* **1985**, *20*, 121–125. (b) Marivet, M. C.; Bourguignon, J.-J.; Lugnier, C.; Mann, A.; Stoclet, J-C.; Wermuth, C-G. Inhibition of Cyclic Adenosine-3′,5′-monophosphate Phosphodiesterase from Vascular Smooth Muscle by Rolipram Analogues. *J. Med. Chem.* **1989**, *32*, 1450–1457.

Scheme II

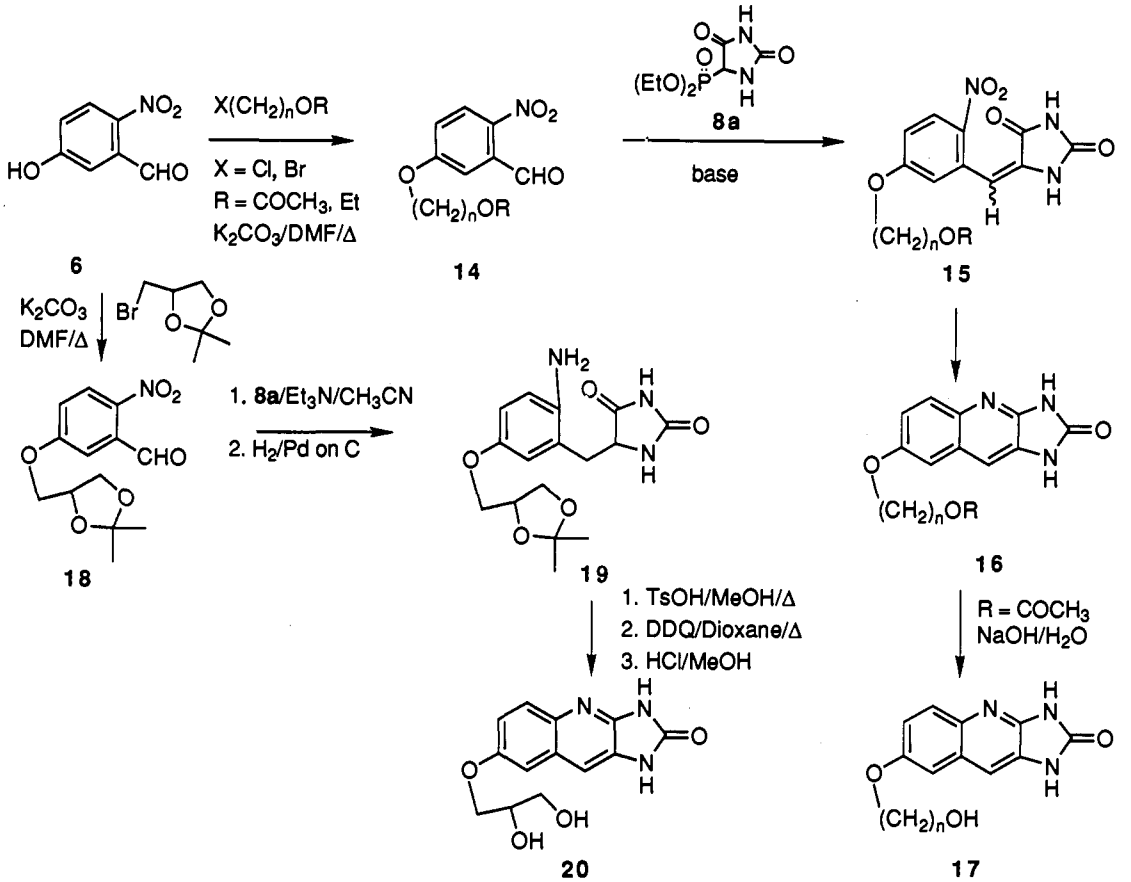

antithrombotic agents, we synthesized a series of 1,3-dihydro-2*H*-imidazo[4,5-*b*]quinolin-2-one derivatives substituted with functionalized side chains capable of interacting with the secondary binding region of the low-K_m cAMP PDE enzyme. In this report, we describe structure–activity relationships associated with this modification which has led to the identification of agents with significantly increased potency compared to the relatively simply substituted compounds disclosed earlier.

Chemistry

On the basis of the structure–activity relationships developed for imidazo[4,5-*b*]quinolin-2-ones[2] and related compounds,[25-27] attachment of the side chain at the 7-position of the heterocycle was considered to be optimal. Scheme I depicts the synthetic approach to a series of 7-oxyalkanoic ester, acid, and amide imidazo[4,5-*b*]-quinolin-2-one derivatives. Alkylation of the commercially-available[30] phenol **6** with an ω-halo ester provided aldehydes **7**,[26] which were reacted with the appropriate hydantoin phosphonate **8**[31] to provide olefins **9**, generally isolated as a mixture of geometrical isomers. The imidazo[4,5-*b*]quinolin-2-one ring system was constructed as previously described[2] by way of exhaustive catalytic reduction of **9** to the racemic anilines **10** followed by cyclization and oxidation using I_2 in MeOH (or EtOH for **10a**) to furnish esters **11**. Methylation of **11e** with methyl iodide, using K_2CO_3 as the base in DMF at 110 °C, gave **11g**. Alkaline hydrolysis of **11** afforded the acids **12**, which were efficiently coupled with amines using DPPA[32] in DMF at room temperature to give amides **13**. The amides **13w** and **13z**, which incorporate an ester functionality, were hydrolyzed to the acids **13y** and **13aa**, respectively, using NaOH in aqueous MeOH. The amides **13a–c** were obtained from ester **11b** by heating with an excess of the appropriate amine in a sealed reaction vessel at 150 °C for several hours.

Alkylation of **6** with ω-bromoalkanol derivatives[27] furnished aldehydes **14**, which were subjected to the standard tricyclic ring construction sequence to afford targets **16**, through the intermediacy of hydantoins **15**, as delineated in Scheme II. By employing CH_3CN as the solvent for cyclization/oxidation of the aniline intermediates analogous to **10**, the acetate moieties in **16b–d** were preserved. Alkaline hydrolysis of **16b–d** provided alcohols **17a–c**. The tosylate of solketal was employed as the electrophile to prepare **18**, which was coupled with phosphonate **8a** and the product hydrogenated over Pd on C to provide racemic aniline **19**. Cyclization of **19**, catalyzed by TsOH in hot MeOH, followed by oxidation using DDQ in dioxane at reflux and dissolution of the product in a 10% solution of

(29) (a) Buchanan, J. O.; Fleming, J. S.; Cornish, B. T.; Baryla, U. M.; Gillespie, E.; Stanton, H. C.; Seiler, S. M.; Keely, S. L. Pharmacology of a Potent, New Antithrombotic Agent, 1,3-Dihydro-7,8-dimethyl-2*H*-imidazo[4,5-*b*]quinolin-2-one (BMY 20844). *Thromb. Res.* **1989**, *56*, 333–346. (b) Seiler, S. M.; Gillespie, E.; Arnold, A. J.; Brassard, C. L.; Meanwell, N. A.; Fleming, J. S. Imidazoquinoline Derivatives: Potent Inhibitors of Platelet cAMP Phosphodiesterase which Elevate cAMP Levels and Activate Protein Kinase in Platelets. *Thromb. Res.* **1991**, *62*, 31–42.

(30) Aldrich Chemical Co., Milwaukee, WI.

(31) Meanwell, N. A.; Roth, H. R.; Smith, E. C. R.; Wedding, D. L.; Wright, J. J. K. Diethyl 2,4-Dioxoimidazolidine-5-phosphonate: A Wadsworth–Emmons Reagent for the Mild and Efficient Preparation of C-5 Unsaturated Hydantoins. *J. Org. Chem.* **1991**, *56*, 6897–6904.

(32) Shioiri, T.; Ninomiya, K.; Yamada, S. Diphenylphosphoryl Azide. A New Convenient Reagent for a Modified Curtius Reaction and for the Peptide Synthesis. *J. Am. Chem. Soc.* **1972**, *94*, 6203–6205.

Scheme III

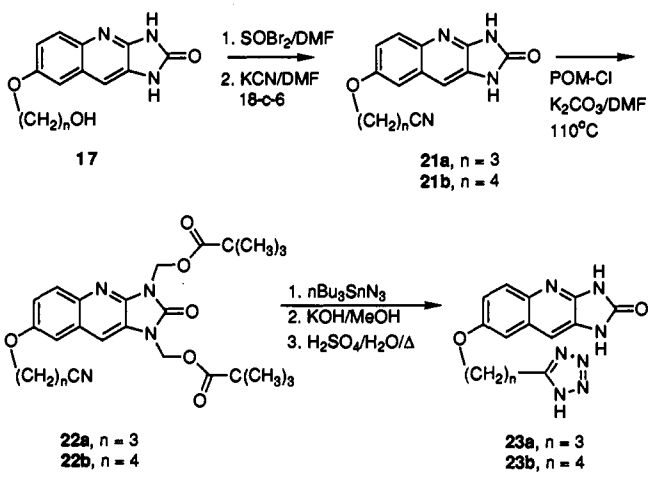

17 21a, n = 3 21b, n = 4

22a, n = 3 22b, n = 4 23a, n = 3 23b, n = 4

Scheme IV

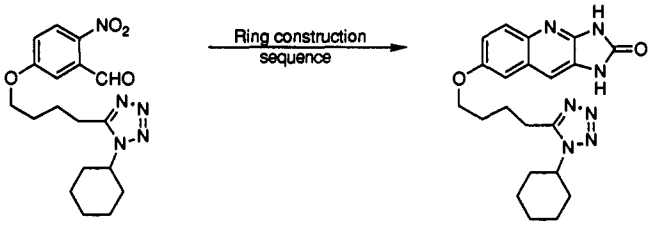

24 25

HCl in MeOH, afforded diol **20**.

The unsubstituted tetrazoles **23** were prepared by the sequence outlined in Scheme III. Bromination of alcohols **17b** and **17c**, using $SOBr_2$ in DMF, provided the corresponding bromides which were converted to nitriles **21a** and **21b** upon heating with KCN in DMF containing a catalytic quantity of 18-crown-6. Attempts to convert nitriles **21** directly to tetrazoles **23** were unsuccessful due to the high melting point and highly insoluble nature of **21**. Alkylation of **21** with (pivaloyloxy)methyl chloride (POM-Cl)[33] in DMF at 110 °C using K_2CO_3 as the base provided the more soluble and lower melting derivatives **22**. These were heated with an excess of nBu_3SnN_3[34] at 105 °C followed by alkaline hydrolysis of the crude material. The final remnants of formaldehyde were removed by heating the products with aqueous H_2SO_4 to afford the tetrazoles **23**. The cyclohexyl-substituted tetrazole **25** was obtained from the known aldehyde **24**[25b] using the standard heterocyclic ring forming sequence as summarized in Scheme IV.

The synthesis of sulfones **29** is outlined in Scheme V. Alkylation of phenol **6** with chlorides **26**[35] furnished the aldehydes **27**, which were elaborated to target compounds **29** through the intermediacy of **28** in the conventional fashion.

The methyl ketone **32** was synthesized as shown in Scheme VI. Alkylation of phenol **6** with the commercially-available[30] chloride **30** furnished aldehyde **31**, which was coupled with phosphonate **8a** and transformed into **32** by the established protocol. The dioxolane protecting group was removed during the final workup procedure after oxidation with iodine by briefly stirring the acidic reaction mixture with water. Reduction of **32** with $NaBH_4$ in DMF gave alcohol **33**.

The 7-hydroxyimidazo[4,5-*b*]quinolin-2-one derivatives prepared as part of this study were generally isolated as high-melting solids and are compiled in Table I.

The synthesis of a series of compounds in which the side chain is attached to the heterocycle by a methylene group rather than an oxygen atom was accomplished as depicted in Scheme VII.[1b] Coupling of the aldehyde **34**[36] with phosphonate **8a** provided adduct **35**,[31] which was hydrogenated over Pd on C and brominated with Br_2 in AcOH at 80 °C to furnish the bromide **36**. The bromination was performed in the presence of NaOAc to trap the HBr produced. Deprotection of **36** in hot ethanolic HCl gave the corresponding aniline which required the unusually vigorous conditions of I_2 in DMF at 150 °C to effect cyclization with concomitant oxidation. Nevertheless, imidazo[4,5-*b*]quinolin-2-one **37** was isolated in high yield and precipitated from the hot reaction mixture as it formed. The extreme insolubility of **37**, mp >310 °C, prevented its participation in Pd-catalyzed Heck-type[37] coupling reactions under a variety of conditions and prompted the development of a strategy for improving the solubility properties of **37** by modifying N-1 and N-3 with ligands more readily removed than the POM moiety employed in the preparation of tetrazoles **23**. Treatment of a suspension of **37** in THF with 2 equiv of NaH and $tBuMe_2SiCl$ at reflux provided the bis-silylated derivative **38**, which was recrystallized from hexanes to give analytically pure material, mp 176–178 °C. The silylated compound **38** exhibits excellent solubility in common organic solvents and is stable to silica gel chromatography but can easily be deprotected in high yield by brief exposure to a catalytic quantity of *p*-TsOH in MeOH at reflux. Pd-catalyzed coupling of **38** with ethyl acrylate or methyl 1,3-butadiene-1-carboxylate[38] provided the adducts **39** which were deprotected to give the unsaturated esters **40a** and **40b**. The large coupling constants observed for the olefinic protons in the ^1H NMR spectra of esters **40a** and **40b** indicated a trans and all-trans geometry, respectively, about the double bonds. Catalytic reduction and subsequent deprotection of **39** provided the saturated esters **41**, which were hydrolyzed to acids **42** under alkaline conditions. Coupling of acids **42** with amines to afford amides **43** was accomplished using DPPA in DMF. The alcohols **44** were obtained from esters **39** by the sequence of hydrogenation over Pd on C followed by reduction, with $LiAlH_4$ in Et_2O, and deprotection.

The 1,3-dihydro-2*H*-imidazo[4,5-*b*]quinolin-2-one derivatives prepared by the procedures summarized in

(33) Rasmussen, M.; Leonard, N. J. The Synthesis of 3-(2′-Deoxy-d-ribofuranosyl)adenine. Application of a New Protecting Group, Pivaloyloxymethyl (Pom). *J. Am. Chem. Soc.* **1967**, *89*, 5439–5444.

(34) Kraus, J. L. Strategies to Synthesize a New Glyphosate Tetrazole Analogue. *Synth. Commun.* **1986**, *16*, 827–832.

(35) Derzhinskii, A. R.; Konyushkin, L. D.; Prilezhaeva, E. N. Functional Sulfur-Containing Compounds. 2. Synthesis of 3-chloropropyl- and 4-chlorobutylalkyl(phenyl)sulfones by the Oxidative Chlorination of 3-Hydroxypropyl- and 4-Hydroxybutylalkyl(phenyl) sulfides and Sulfoxides. *Izv. Akad. Nauk. SSSR, Ser. Khim.* **1978**, *9*, 2070–2076; *Chem. Abstr.* **1979**, *90*, 38501*k*.

(36) Ortho N-acetyl benzaldehyde was prepared from 2-nitrobenzaldehyde by the sequence of protection (ethylene glycol/*p*-TsOH/toluene/Δ), reduction (10% Pd on C/EtOAc), and acetylation (CH_3COCl/pyridine/CH_2Cl_2).

(37) Heck, R. F. Palladium-Catalyzed Vinylation of Organic Halides. *Org. React.* **1982**, *27*, 345–390.

(38) Purchased from Fluka Chem. Corp., Ronkunkoma, NY.

(39) Neanwell, N. A.; Rosenfeld, M. J.; Wright, J. J. K.; Brassard, C. L.; Buchanan, J. O.; Federici, M. E.; Fleming, J. S.; Seiler, S. M. Structure–Activity Relationships Associated with 3,4,5-Triphenyl-1*H*-pyrazole-1-nonanoic Acid, a Nonprostanoid Prostacyclin Mimetic. *J. Med. Chem.* **1992**, *35*, 389–397.

Scheme V

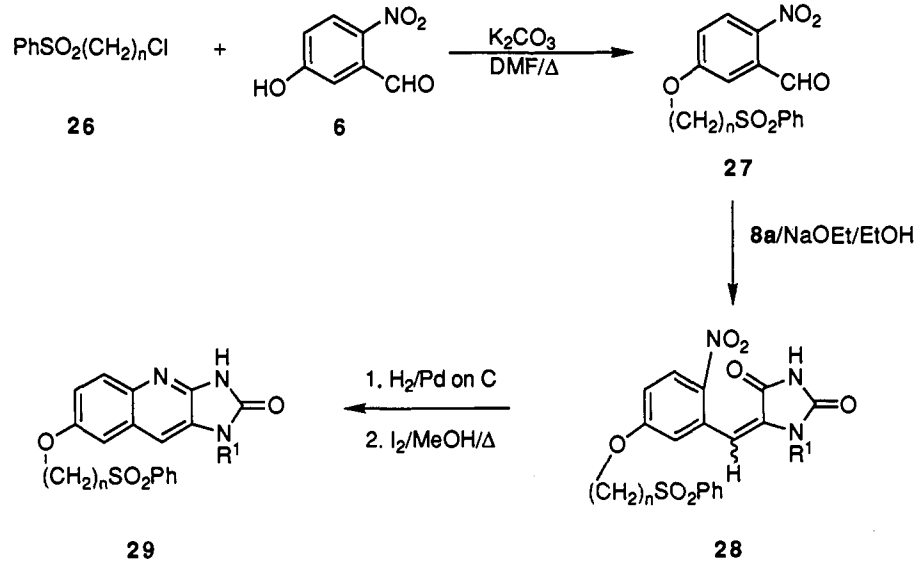

Scheme VI

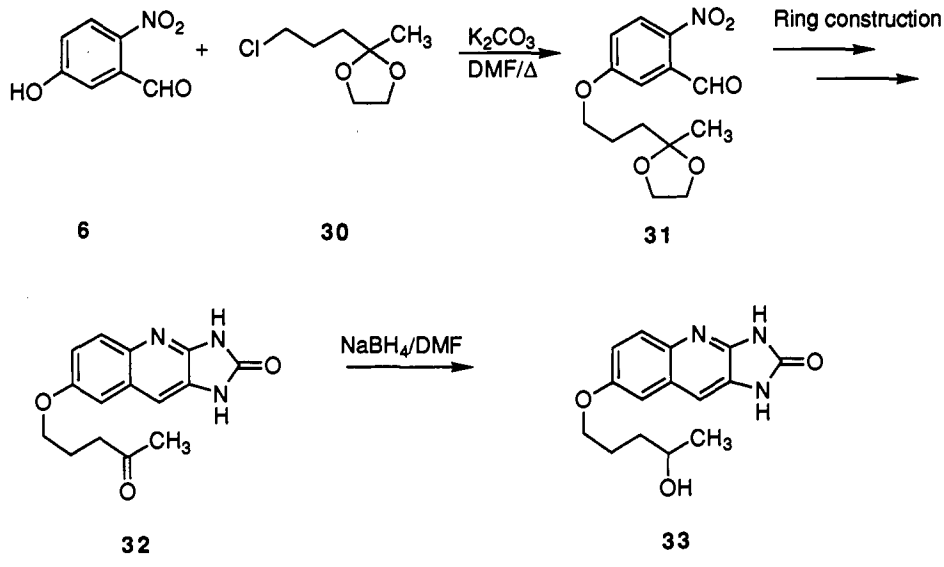

Scheme VII are listed in Table II along with pertinent physical properties.

Samples of ester **45** and acid **46** were synthesized as described[26] for comparative purposes. Lixazinone (**4**) was prepared, albeit in poor yield, from acid **46** and *N*-methyl-*N*-cyclohexylamine by treatment with DPPA in DMF at room temperature.

Biological Evaluation

The target compounds were evaluated as inhibitors of cAMP and cGMP hydrolysis using a dilute human platelet sonicate with 0.15 μM cAMP or 0.25 μM cGMP according to methods previously described.[24b,29b] The concentrations of test compound that inhibited PDE activity to 50% of control were determined from dose–response curves and are reported in Table III. In this assay, anagrelide (**2**) displayed IC_{50}'s of $(5.4 \pm 1.4) \times 10^{-8}$ M vs cAMP and $(34 \pm 7) \times 10^{-6}$ M vs cGMP.[24b] Platelet inhibitory activity was determined in rabbit platelet-rich plasma (PRP) using ADP and collagen as the activating agents or in human PRP using ADP as the stimulating agent, as previously described.[2,29a] Dose–response curves were obtained, and the results are expressed as the concentration of drug necessary to prevent aggregation by 50% compared to drug-free controls. The data compiled in Table III are the result of a single determination or the average of duplicates. Anagrelide, employed as a positive reference agent in these evaluations, displayed EC_{50}'s of 1.05 ± 0.27 μM vs ADP and 0.27 ± 0.07 μM vs collagen in rabbit PRP and 1.05 ± 0.3 μM vs ADP in human PRP. A measure of oral efficacy of drug candidates was determined in rats using the ex vivo aggregometry protocol described previously.[2] ED_{50}'s, in milligrams/kilogram, are reported in Table III.

Results and Discussion

It is apparent from an examination of the data presented in Table III that the introduction of a functionalized side chain at the 7-position of the imidazo[4,5-*b*]quinolin-2-one heterocycle exerts a profound effect on biological activity. cAMP PDE and blood platelet inhibitory potency varies by over 6000-fold across the series of side-chain modifications examined and intrinsic activity is dependent upon the identity of the terminal functionality and its relationship with the heterocycle. In those cases where comparisons can be made, the compounds listed in Table III are highly selective inhibitors of cAMP degradation by the platelet enzyme, a profile intrinsic to this structural class.[2] However, whereas inhibition of agonist induced blood platelet aggregation for relatively simply substituted imidazo[4,5-*b*]quinolin-2-one derivatives correlated with

Scheme VII

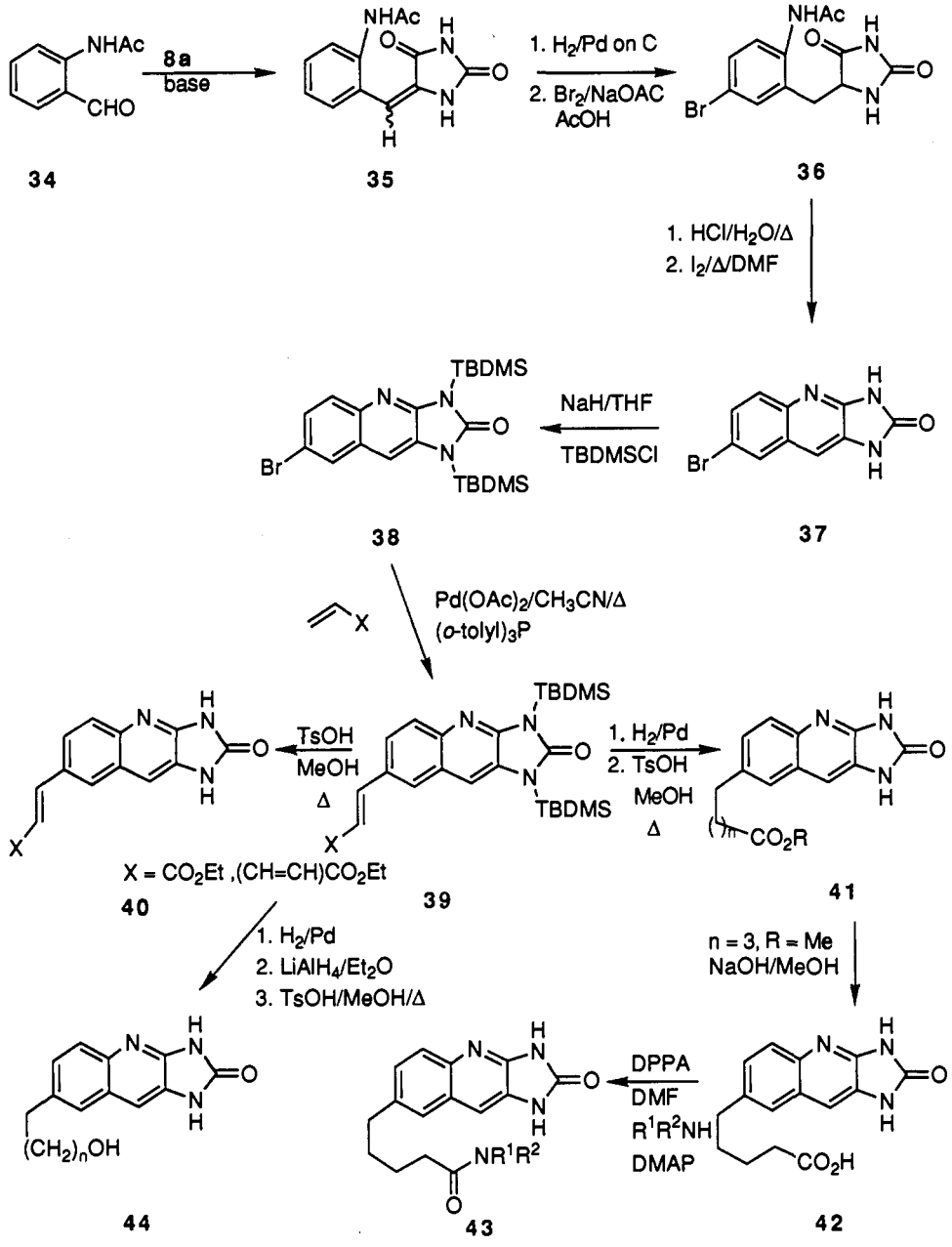

cAMP PDE inhibitory activity,[2] this is clearly not the case for several examples presented in Table III.

For the series of esters **11a–j**, cAMP PDE inhibitory activity is dependent on side-chain length with the pentanoate **11h** optimal and the hexanoate **11j**, butyrate **11b**, and acetate **11a** exhibiting decreased activity, respectively. Ester identity also influences potency within the butyrate series **11b–d** with Et > ^{i}Pr = Me. While esterases may be present in the PDE assay medium, this SAR coupled with the fact that the corresponding acid **12b** is significantly more potent than **11b–d** (vide infra) suggests that the observed inhibitory activity is due to the parent esters. Replacement of the concatenating O atom of acetate **11a** with a CH_2 (**41a**) results in a small increase in potency that is reversed by introducing unsaturation (**40a**). In contrast, an analogous O to CH_2 modification for the homologue **11b** is associated with a 2-fold reduction in potency (**41b**) but increasing side-chain rigidity leads to a marked enhancement in PDE inhibitory activity. The all-trans pentadienoate **40b** is 1 order of magnitude more potent than pentanoate **41b**, presumably reflecting a favorable entropic contribution to the binding event. Furthermore, if effective and extended π overlap is assumed for **40b** when bound to the enzyme, some limitations are readily apparent concerning the location of the side-chain terminus relative to the heterocycle. Of the four possible energetically most stable conformations, that shown in Figure 2 most closely approximates the model favored by Venuti.[27]

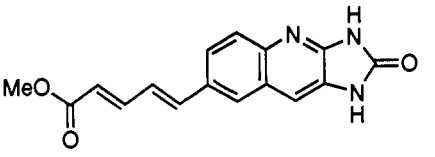

Figure 2. Conformation of **40b**.

Methylation at N-1 (**11e**), N-3 (**11f**), or N-1 and N-3 (**11g**) of the heterocycle reduces cAMP PDE inhibitory activity by at least 1 order of magnitude, in parallel with earlier observations.[2]

The cAMP PDE inhibitory properties of the carboxylic acids **12a–h** and **42** demonstrates a similar dependence on

Table I. Structure and Physical Properties of 7-Hydroxyimidazo[4,5-*b*]quinolin-2-one Derivatives

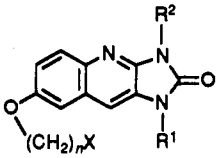

no.	R^1	R^2	*n*	X	mp, °C	mol formula (elem anal)
11a	H	H	1	CO_2Et	304–306	$C_{14}H_{13}N_3O_4 \cdot HCl \cdot 0.3H_2O$
11b	H	H	3	CO_2Me	297–299	$C_{15}H_{15}N_3O_4$
11c	H	H	3	CO_2Et	276–278	$C_{16}H_{17}N_3O_4$
11d	H	H	3	$CO_2{}^iPr$	263–265	$C_{17}H_{19}N_3O_4 \cdot 0.5H_2O$
11e	CH_3	H	3	CO_2Me	222–224	$C_{16}H_{17}N_3O_4$
11f	H	CH_3	3	CO_2Me	210–220	$C_{16}H_{17}N_3O_4 \cdot HCl$
11g	CH_3	CH_3	3	CO_2Me	202–204	$C_{17}H_{19}N_3O_4 \cdot HCl$
11h	H	H	4	CO_2Me	281–282	$C_{16}H_{17}N_3O_4$
11i	CH_3	H	4	CO_2Me	223–225	$C_{17}H_{19}N_3O_4$
11j	H	H	5	CO_2Me	275–276.5	$C_{17}H_{19}N_3O_4 \cdot 0.05H_2O$
12a	H	H	1	CO_2H	340–342 dec	$C_{12}H_{19}N_3O_4 \cdot 0.15H_2O$
12b	H	H	3	CO_2H	327–330	$C_{14}H_{13}N_3O_4$
12c	CH_3	H	3	CO_2H	286–288.5	$C_{15}H_{15}N_3O_4$
12d	H	CH_3	3	CO_2H	305–307	$C_{15}H_{15}N_3O_4$
12e	CH_3	CH_3	3	CO_2H	206–208	$C_{16}H_{17}N_3O_4 \cdot 0.2H_2O$
12f	H	H	4	CO_2H	317–318	$C_{15}H_{15}N_3O_4$
12g	CH_3	H	4	CO_2H	311–313	$C_{16}H_{17}N_3O_4$
12h	H	H	5	CO_2H	313–315	$C_{16}H_{17}N_3O_4$
13a	H	H	3	$CONH_2$	328–331	$C_{14}H_{14}N_4O_3 \cdot 0.65H_2O$
13b	H	H	3	CONHMe	317–319	$C_{15}H_{16}N_4O_3$
13c	H	H	3	$CONMe_2$	292–294	$C_{16}H_{19}N_4O_3$
13d	H	H	3	CONMe-c-C_6H_{11}	198–201	$C_{21}H_{26}N_4O_3 \cdot HCl \cdot 0.4H_2O$
13e	CH_3	H	3	CONMe-c-C_6H_{11}	218–220	$C_{22}H_{28}N_4O_3 \cdot 0.4H_2O$
13f	H	H	4	CONMe-c-C_6H_{11}	207–210	$C_{22}H_{28}N_4O_3 \cdot 0.11H_2O$
13g	CH_3	H	4	CONMe-c-C_6H_{11}	190–192	$C_{23}H_{30}N_4O_3 \cdot 0.1H_2O$
13h	H	H	5	CONMe-c-C_6H_{11}	223–227	$C_{23}H_{30}N_4O_3$
13i	H	CH_3	3	CONMe-c-C_6H_{11}	178–184 dec	$C_{22}H_{28}N_4O_3 \cdot 2HCl \cdot 0.3H_2O$
13j	CH_3	CH_3	3	CONMe-c-C_6H_{11}	185–190	$C_{23}H_{30}N_4O_3 \cdot 0.1H_2O$
13k	H	H	3	CONMe-c-C_7H_{13}	180–182	$C_{22}H_{28}N_4O_3 \cdot HCl$
13l	CH_3	H	3	CONMe-c-C_7H_{13}	234.5–236.5	$C_{23}H_{30}N_4O_3$
13m	H	H	4	CONMe-c-C_7H_{13}	189–191	$C_{23}H_{30}N_4O_3 \cdot 0.15H_2O$
13n	CH_3	H	4	CONMe-c-C_7H_{13}	183–185	$C_{24}H_{32}N_4O_3 \cdot 0.1H_2O$
13o	H	H	3	$CONHC_5H_9$	>320	$C_{19}H_{22}N_4O_3$
13p	H	H	3	CONH-c-C_6H_{11}	>320	$C_{20}H_{24}N_4O_3$
13q	CH_3	H	3	CONH-c-C_6H_{11}	282–284	$C_{21}H_{26}N_4O_3$
13r	H	H	3	CONH-c-C_7H_{13}	314–316	$C_{21}H_{26}N_4O_3$
13s	H	H	3	CONH-1-adamantanyl	304–306 dec	$C_{24}H_{28}N_4O_3$
13t	H	H	3	CO-1-piperidinyl	284.5–285.5	$C_{19}H_{22}N_4O_3$
13u	CH_3	H	3	CO-1-piperidinyl	215–217	$C_{20}H_{24}N_4O_3$
13v	H	H	3	CO-4-morpholinyl	274–276	$C_{18}H_{20}N_4O_4$
13w	H	H	3	CON-c-$C_6H_{11}CH_2CO_2Me$	215–218	$C_{23}H_{28}N_4O_5 \cdot 0.25H_2O$
13x	H	H	3	CON-c-$C_6H_{11}CH_2CO_2Et$	199–201	$C_{24}H_{30}N_4O_5 \cdot 0.2H_2O$
13y	H	H	3	CON-c-$C_6H_{11}CH_2CO_2H$	254–258 dec	$C_{22}H_{26}N_4O_5 \cdot 0.15DMF$
13z	H	H	3	$CON(CH_2CH_2)_2CHCO_2Et$	251–253	$C_{22}H_{26}N_4O_5$
13aa	H	H	3	$CON(CH_2CH_2)_2CHCO_2H$	278–280 dec	$C_{20}H_{22}N_4O_5$
16a	H	H	2	OEt	290–293	$C_{14}H_{15}N_3O_3 \cdot HCl$
16b	H	H	2	OCOMe	299–302 dec	$C_{14}H_{13}N_3O_4$
16c	H	H	3	OCOMe	301–303	$C_{15}H_{15}N_3O_4$
16d	H	H	4	OCOMe	277–279	$C_{16}H_{17}N_3O_4$
17a	H	H	2	OH	>320	$C_{12}H_{11}N_3O_3$
17b	H	H	3	OH	343–345	$C_{13}H_{13}N_3O_3$
17c	H	H	4	OH	306–309	$C_{14}H_{15}N_3O_3$
20	H	H	1	$C(OH)CH_2OH$	258–261	$C_{13}H_{13}N_3O_4 \cdot HCl$
21a	H	H	3	CN	328–332 dec	$C_{14}H_{12}N_4O_2 \cdot 0.1CH_3OH$
21b	H	H	4	CN	308–311 dec	$C_{15}H_{14}N_4O_2 \cdot 0.4CH_3OH \cdot 0.1DMF$
23a	H	H	3	CN_4H	295–324 dec	$C_{14}H_{13}N_7O_2 \cdot 0.07DMF$
23b	H	H	4	CN_4H	299–301	$C_{15}H_{15}N_7O_2 \cdot 0.6DMF \cdot 0.1H_2O$[a]
25	H	H	4	CN_4-c-C_6H_{11}	288–291	$C_{21}H_{25}N_7O_2 \cdot HCl$
29a	H	H	3	SO_2Ph	284–287 dec	$C_{19}H_{17}N_3O_4S$
29b	CH_3	H	3	SO_2Ph	245–247 dec	$C_{20}H_{19}N_3O_4S$
29c	H	H	4	SO_2Ph	267–268 dec	$C_{20}H_{19}N_3O_4S$
32	H	H	3	$COCH_3$	294–296	$C_{15}H_{15}N_3O_3 \cdot 0.12H_2O$
33	H	H	3	$CH(OH)CH_3$	301–303	$C_{15}H_{17}N_3O_3$

[a] N: calcd, 28.69; found, 28.26.

side-chain length, methylation of the nucleus, and side-chain concatenation to that observed for the esters **11a–j** and **41b**. However, the acids **12** and **42** are at least 1 order of magnitude more potent than the corresponding methyl esters. More specifically, **12b**, **12f**, and **12h** half-maximally inhibit cAMP PDE at low nM concentrations, demon-

Table II. Structure and Physical Properties of 7-Carbon-Substituted Imidazo[4,5-b]quinolin-2-one Derivatives

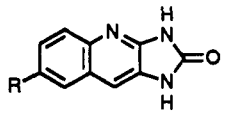

no.	R	mp, °C	mol formula (elem anal.)
40a	CH=CHCO$_2$Et	>310	$C_{15}H_{13}N_3O_3$
40b	CH=CHCH=CHCO$_2$Me	>310	$C_{16}H_{13}N_3O_3 \cdot 0.1H_2O$
41a	(CH$_2$)$_2$CO$_2$Et	292–294	$C_{15}H_{15}N_3O_3$
41b	(CH$_2$)$_4$CO$_2$Me	293–295	$C_{16}H_{17}N_3O_3$
42	(CH$_2$)$_4$CO$_2$H	>310	$C_{15}H_{15}N_3O_3$
43a	(CH$_2$)$_4$CONMe-c-C$_6$H$_{11}$	196–198	$C_{22}H_{28}N_4O_2 \cdot 0.1H_2O$
43b	(CH$_2$)$_4$CONH-c-C$_6$H$_{11}$	>315	$C_{21}H_{26}N_4O_2 \cdot 0.1DMF$
43c	(CH$_2$)$_4$CONH-1-adamantanyl	298–300	$C_{25}H_{30}N_4O_2$[a]
43d	(CH$_2$)$_4$CO-1-piperidinyl	240–242	$C_{20}H_{24}N_4O_2 \cdot 0.1H_2O$
44a	(CH$_2$)$_3$OH	>310	$C_{13}H_{13}N_3O_2$
44b	(CH$_2$)$_5$OH	>310	$C_{15}H_{17}N_3O_2$

[a] C: calcd, 71.74; found, 70.31.

strating a tolerance and perhaps some preference for an ionizable functionality at this region of the pharmacophore.

The platelet inhibitory properties of the esters **11**, **40**, and **41** and acids **12** and **42** provide some interesting structure–activity relationships that reveals a departure from the correlation with cAMP PDE inhibition observed for simpler compounds. Compared to results obtained in the earlier studies,[2] the methyl ester **11b** is a more potent inhibitor of ADP- and collagen-induced aggregation in rabbit PRP than might be anticipated on the basis of the efficacy with which this compound inhibits cAMP PDE. The esters **11h** and **11j** show a similar but less marked proclivity. This observation may be due to the presence of significant amounts of the corresponding acids **12b**, **12f**, and **12h**, respectively, which are considerably more potent cAMP PDE inhibitors than the methyl esters, produced inside the platelet during the 3-min incubation period prior to addition of the agonist. Consistent with this suggestion, increasing the size of the methyl ester of **11b** to the metabolically more stable ethyl (**11c**) and isopropyl (**11d**) moieties leads to a marked diminution in platelet inhibitory activity when ADP is used as the agonist, although this trend is less pronounced when collagen is the activating agent. In contrast, the hierarchy with respect to ester identity is reversed in the human PRP assay such that ^{i}Pr > Et > Me, a finding that may reflect subtle variations in the coalescence of intrinsic cAMP PDE inhibitory activity, membrane permeability, and individual susceptibility to ester cleavage. Within the ester series **11**, alkylation at N-1 and/or N-3 and substitution of the side chain O by CH_2 is associated with reduced platelet inhibitory activity, a trend that parallels cAMP PDE inhibition.

The platelet inhibitory properties of the carboxylic acids **12** reveals an SAR that is critically dependent on side-chain length. Activity is optimal with the butyrate **12b** and only the doubly homologated congeners, acetate **12a** and hexanoate **12h**, exhibit significant inhibitory effects in the rabbit PRP assay. Homologation of the side chain of **12b** by a single atom (**12f**) or methylation at N-1 (**12c**) results in greater than a 100-fold decline in potency, despite the complete retention of cAMP PDE inhibitory activity in the case of **12f**. This suggests that the acids **12c** and **12f** are denied access to the platelet interior under the constraints of the assay and are unable to express their cAMP PDE inhibitory properties. Since it is unlikely that such minor structural variations would significantly alter passive membrane diffusivity, the platelet inhibitory activity associated with acids **12a**, **12b**, and **12h** may be the result of either a facilitated membrane permeability or drug action at an extracellular site. Exposure of human platelets to **12b** results in an increase in intracellular cAMP levels and activation of the cAMP-dependent protein kinase, but **12b** does not stimulate adenylate cyclase in a platelet membrane preparation.[40] Although these data are consistent with acid **12b** expressing platelet inhibitory activity via inhibition of cAMP PDE, interference with other platelet regulatory pathways cannot be ruled out. Indeed, a non-cAMP PDE-dependent mechanism of action for acid **12b** would provide an alternative explanation for the high level of platelet inhibitory activity observed with ester **11b**. Thus, esterase-mediated production of significant quantities of the acid **12b** from methyl ester **11b** in PRP during the 3-min incubation period could result in activation of an inhibitory pathway that may interact synergistically with inhibition of cAMP PDE by the intact ester.[41] Whatever the mode of action of acids **12a**, **12b**, and **12h**, platelet inhibitory activity is exquisitely sensitive to side-chain length and methylation at N-1 of the heterocycle as well as heterocycle variation, since acids **12c**, **12e** and **46** and **47**[25a] are ineffective platelet aggregation inhibitors. Replacement of the side chain O atom of **12b** by CH_2 leads to a compound (**42**) 60-fold weaker in the rabbit platelet assay, whereas methylation at N-3 is tolerated since **12d** retains activity. Some species dependence is also apparent since acid **12b** is 1 order of magnitude less potent in human PRP compared to rabbit PRP while the N-3 methylated congener **12d** is at least 20-fold less effective.

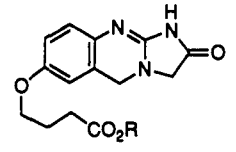

45 R = Et

46 R = H

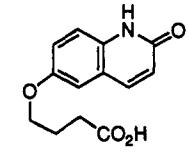

47

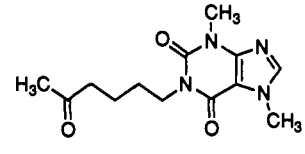

48, Pentoxifylline

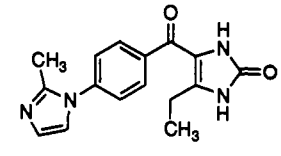

49

The amide derivatives **13** are a family of very potent inhibitors of platelet cAMP PDE that would be expected to be metabolically more stable than the esters **11**. Several structure–activity trends within this series of compounds are apparent from the data presented in Table III. Variation of the amide moiety influences potency and tertiary amide derivatives are generally more potent inhibitors of platelet cAMP PDE than either secondary or cyclic amides, which exhibit similar efficacy. The high potency of secondary amide **13b** is reduced as the size of the N-substituent is increased (**13o,p,r**), except when the substituent is a very lipophilic adamantyl moiety (**13s**). In contrast, replacing one of the methyl groups of dimethylamide **13c**

(40) Grove, R. I.; Seiler, S. M. Unpublished studies.

(41) A combination of acid **12b** and a derived amide were found to interact in a synergistic fashion to inhibit ADP-induced aggregation of human platelets in vitro (Fleming, J. S.; Buchanan, J. O. Unpublished observations).

by a cyclohexyl (**13d**) or cycloheptyl (**13k**) ring leads to a 10-fold increase in potency. The introduction of additional polar functionality into the amide terminus results in a further enhancement in potency both in an acyclic (**13w**, **13x**) and cyclic (**13z**) configuration. Homologation of the side chain of the butyrate derivatives **13d** and **13k** by 1 or 2 atoms produces only minor variations in potency but replacement of the C-7 ethereal oxygen atom of **13d**, **13p**, **13s**, and **13t** by a CH_2 led to compounds (**43a–d**) with reduced activity. The C-7 oxygen atom may function as the hydrogen bond accepting moiety postulated at this region of the cAMP PDE inhibitor pharmacophore.[22] Without exception, methylation of either N-1 and/or N-3 of the heterocycle results in compounds at least 1 order of magnitude weaker as inhibitors of cAMP PDE than their N–H counterparts.

The platelet inhibitory activity of amides **13** demonstrates a broad variation in potency with the more lipophilic side-chain termini generally associated with increased activity. This presumably reflects differences in membrane diffusivity and is consistent with the notion of an optimum lipophilic window for efficient drug delivery.[26,27] The simple amides **13a–c** are comparatively weak inhibitors of ADP- and collagen-induced rabbit platelet aggregation, only marginally more effective than the unsubstituted parent heterocycle[2] despite being substantially more potent cAMP PDE inhibitors. Increasing the lipophilicity of the amide moiety results in a dramatic (100–1000-fold) enhancement of platelet inhibitory activity and several representatives of **13** are among the most potent, non-prostanoid platelet aggregation inhibitors yet described. For example, **13d**, which incorporates the cilostamide-type side chain, half-maximally inhibits ADP- and collagen-induced platelet aggregation at low nM concentrations. Compared to RS 82856 (**4**), **13d** is 20–60-fold more potent even though the two agents are equieffective cAMP PDE inhibitors. Presumably the more basic heterocyclic nucleus of **4** interferes with efficient trans-membrane delivery compared to **13d**.[42] The butanoate (**13d**) and pentanoate (**13f**) side chain variants within this series are of comparable potency in the platelet aggregation assays, but the single hexanoate, **13h**, is less effective. In parallel with the effects on cAMP PDE inhibition, methylation of the heterocyclic nitrogen atoms results in weaker inhibitors of platelet aggregation. However, the N-1 methylated amides **13e**, **13g**, **13l**, and **13n** are, nevertheless, potent platelet aggregation inhibitors. The N-3 methylated amide **13i** demonstrates a pattern of species-dependent[44] platelet inhibitory activity that appears to be a hallmark of this class of cAMP PDE inhibitor. Thus, **13i**, **11f**, and **12d** are all effective inhibitors of ADP- and collagen-induced aggregation of rabbit blood platelets but are much less efficacious in human PRP, a phenomenon noted in the earlier study that may reflect differences in human and rabbit cAMP PDE architecture.[2]

The potent PDE inhibitory activity of ester **13w** is very effectively expressed in the whole cell environment where it is an exceptionally potent broad spectrum inhibitor of platelet aggregation with potency comparable to that of prostacyclin.[39] However, in the two examples where an ester moiety is incorporated into the amide terminus (**13w** and **13z**), the corresponding acids (**13y** and **13aa**, respectively) are less effective platelet aggregation inhibitors. This is most dramatically exemplified by comparing the effects of ester **13w** with acid **13y** as inhibitors of ADP-induced aggregation in human PRP. The acid **13y** is 13 000-fold less potent than ester **13w** under these circumstances, despite similarly effective cAMP PDE inhibition by the two agents.

The functional demands of the secondary binding region were further probed with the evaluation of several structural variants of the side-chain terminus. Within the series of alcohols **17**, optimal cAMP PDE inhibitory activity is observed with an extended chain (**17b** and **17c**) that is weakened upon acetylation (**16c** and **16d**), possibly reflecting the presence of hydrogen bond accepting functionality in the enzyme. Glycol derivative **17a** is the most potent platelet aggregation inhibitor in this series, with human PRP particularly sensitive, but alkylation (**16a**) or acetylation (**16b**) diminishes activity. Diol **20**, a structural hybrid of **17a** and **17c**, is equipotent with **17a** as a cAMP PDE inhibitor but a much less effective inhibitor of platelet aggregation. The increased hydrophilicity of **20** presumably interferes with drug delivery to the target enzyme.

Potent cAMP PDE inhibition is retained with a nitrile terminus (**21**) but activity is dependent on side-chain length (butyronitrile **21a** > pentanenitrile **21b**) and this is reflected in the aggregometry screen. The tetrazoles **23a** and **23b** are potent PDE inhibitors with activity comparable to that of the analogous acids **12b** and **12f**, respectively, with which they are isosteric.[45] Interestingly, in contrast to the observations with the acids **12b** and **12f**, both tetrazoles **23a** and **23b** inhibit platelet aggregation in rabbit PRP, where they are virtually equipotent. While the platelet inhibitory effect of tetrazole **23b** suggests increased membrane diffusivity compared to the analogous acid **12f**, the data are also compatible with the alternative mechanistic proposals considered above for the acids **12**. The structure–activity relationships for either a non-cAMP PDE-dependent mechanism or facilitated membrane permeability can be reconciled by assuming that the tetrazole ring of **23a** is an imperfect surrogate for the carboxylic acid moiety in butyrate **12b** and that, by virtue of delocalization, tetrazole **23b** is an effective mimic of hexanoic acid **12h**. The diminished activity of tetrazoles **23** in human PRP further highlights variations between species.[44]

Substitution of N-1 of the tetrazole ring of **23b** with a cyclohexyl group provides a compound, **25**, that is only incrementally more potent in the cAMP PDE assay but is a much more efficient platelet inhibitor. However, this side-chain configuration, which is identical to that found in the clinically evaluated cAMP PDE inhibitor cilostazole,[46] is considerably less effective than the similarly substituted amides **13f** and **13m**.

Within the concise series of phenyl sulfones **29**, potent cAMP PDE inhibitory activity is observed with **29a** that is not significantly influenced by side-chain length. However, the more lipophilic homologue **29c** is the more

(42) The pK_a of a protonated imidazo[4,5-*b*]quinolin-2-one derivative related to **13d** has been measured as 1.9 (Paborji, M. Unpublished data) compared to a pK_a of 3.5 reported for lixazinone.[43]

(43) Visor, G. C.; Lin, L-H.; Benjamin, E.; Strickley, R. G.; Gu, Lu. Parenteral Formulation Development for the Positive Inotropic Agent RS-82856: Solubility and Stability Enhancement Through Complexation and Lyophilization. *J. Parenter. Sci. Technol.* **1987**, *41*, 120–125.

(44) Hwang, D. H. Species Variation in Platelet Aggregation. *The Platelets. Physiology and Pharmacology*; Longenecker, G. L., Ed.; Academic Press, Inc.: Orlando, 1985; Chapter 12.

(45) Thornber, C. W. Isosterism and Molecular Modification in Drug Design. *Chem. Soc. Rev.* **1979**, *8*, 563–580.

(46) For a comprehensive review of the preclinical profile and early clinical studies of cilostazole, see: *Arzneim. Forsch.* **1985**, *35*, 1117–1208.

Table III. Biological Evaluation of Imidazo[4,5-*b*]quinolin-2-one Derivatives and Imidazo[2,1-*b*]quinazolin-2-ones **4**, **45**, and **46**

no.	inhibition of human platelet phosphodiesterase: IC_{50}, μM[a]		inhibition of platelet aggregation: EC_{50}, μM[b]			rat exo vivo vs ADP: ED_{50}, mg/kg[c]
			rabbit PRP		human PRP	
	vs cAMP	vs cGMP	vs ADP	vs collagen	vs ADP	
5	0.01	20	0.39	0.12	0.02	3.2
11a	2.0	NT	24.3	7.6	NT	
11b	0.4	>100	0.066	0.02	0.083	4.4
11c	0.02	NT	0.63	0.063	0.038	
11d	0.3	NT	0.59	0.021	0.012	>10 (24%)
11e	7.0	100	1.9	0.25	NT	
11f	2.0	NT	0.36	0.17	29.85	
11g	40.0	NT	>87.5	54.7	NT	
11h	0.03	>100	0.95	0.095	NT	>10
11i	5.0	100	9.11	0.61	NT	
11j	0.06	>100	0.09	0.027	NT	
12a	0.07	50	1.91	0.76	NT	<10 (61%)
12b	0.005	30	1.04	0.35	14.97	3.4
12c	0.6	10	>106	>106	NT	>10
12d	1.0	NT	1.66	0.1	>26.5	<10 (59%)
12e	4.0	NT	9.41	1.25	>100	
12f	0.005	30	>106	>106	>106	
12g	0.08	10	>100	>100	NT	
12h	0.004	7	3.17	0.95	NT	
13a	0.008	>100	6.04	2.52	3.02	
13b	0.007	NT	1.33	0.83	71.6	<10 (57%)
13c	0.04	NT	4.77	0.95	0.19	>10
13d	0.002	6	0.005	0.002	0.007	2.9
13e	0.2	8	0.05	0.04	NT	2.1
13f	0.002	5	0.008	0.0002	0.001	3.8
13g	0.5	60	0.15	0.07	NT	10
13h	0.003	7	0.02	0.006	0.54	
13i	0.1	NT	0.52	0.13	33	<10 (68%)
13j	5.0	NT	26.7	13.4	NT	
13k	0.003	NT	0.016	0.005	NT	6.2
13l	0.1	7	0.07	0.01	1.22	10
13m	0.0004	5	0.005	0.002	0.001	1.7
13n	0.6	10	0.14	0.07	0.54	>10 (43%)
13o	0.02	NT	0.42	0.004	NT	
13p	0.03	>100	0.04	0.007	NT	>10 (31%)
13q	0.7	>100	0.18	0.02	7.84	8.3
13r	0.01	NT	0.39	0.008	0.016	5.4
13s	0.001	100	0.12	0.05	0.02	4
13t	0.02	>100	0.11	0.08	0.13	<10 (57%)
13u	2.0	60	10.86	2.44	NT	
13v	0.04	40	0.28	0.02	NT	>10
13w	0.0005	5.5	0.006	0.002	0.0007	3
13x	0.002	3	0.02	0.009	0.08	
13y	0.0003	NT	0.91	0.46	9.60	
13z	0.005	100	0.21	0.09	0.09	9.6
13aa	0.02	NT	0.38	0.18	45.28	
16a	0.05	NT	4.84	1.29	NT	
16b	0.03	NT	0.87	0.07	NT	
16c	0.1	NT	0.33	0.03	NT	
16d	0.04	NT	0.95	0.32	NT	
17a	0.02	>100	0.02	0.004	0.004	<10
17b	0.009	50	0.77	0.15	NT	
17c	0.006	20	0.055	0.033	0.09	>10 (47%)
20	0.02	NT	0.26	0.064	11.87	
21a	0.006	NT	0.18	0.033	0.60	
21b	0.1	NT	1.32	0.13	NT	
23a	0.003	NT	6.32	1.58	>100	
23b	0.01	NT	5.40	1.01	51	
25	0.004	>100	0.25	0.045	NT	>10 (44%)
29a	0.002	>100	0.39	0.05	NT	
29b	0.3	NT	50.3	15.1	NT	
29c	0.001	>100	0.18	0.075	0.01	4.3
32	0.08	NT	1.40	0.07	NT	
33	0.1	NT	0.52	0.07	0.1	
40a	1.0	NT	0.44	0.28	NT	
40b	0.09	NT	2.69	0.67	NT	10
41c	0.6	NT	0.44	0.14	NT	
41b	0.9	NT	0.43	0.27	3.0	>10 (29%)
42	0.02	10	63.1	21.0	>112	
43a	0.04	NT	0.21	0.026	1.1	
43b	0.3	NT	1.07	0.19	49.5	
43c	0.006	NT	0.96	0.30	5.26	
43d	0.06	NT	0.42	0.17	15.52	

Table III (Continued)

no.	inhibition of human platelet phosphodiesterase: IC_{50}, μM[a]		inhibition of platelet aggregation: EC_{50}, μM[b]			rat exo vivo vs ADP: ED_{50}, mg/kg[c]
			rabbit PRP		human PRP	
	vs cAMP	vs cGMP	vs ADP	vs collagen	vs ADP	
44a	0.06	NT	2.47	0.41	NT	
44b	0.1	NT	2.95	0.22	NT	>10 (26%)
45	0.07	NT	NT	NT	NT	
46	0.04	NT	6.91	3.46	>100	
4	0.003	NT	0.1	0.08	0.44	

[a] IC_{50} values were obtained from plots of cAMP hydrolysis versus concentration of test compound in the assay and the data presented is the average of duplicate determinations. BMY 20844 (5) $IC_{50} = (1.3 \pm 0.6) \times 10^{-8}$ M vs cAMP,[5] was used as a positive control. [b] Data shown are the result of a single or the average of duplicate determinations with anagrelide, $IC_{50} = 1.05 \pm 0.3$ μM, used as a reference agent. Standard incubation time of PRP with drug prior to the addition of ADP was 3 min. [c] Figures in parentheses are percent inhibition at 10 mg/kg.

Table IV. Inhibition of Thrombus Formation in the Conscious Rabbit by cAMP PDE Inhibitors

dose, mg/kg po	mean thrombus area, $\mu M^2 \pm SE$[a] (% inhibition of thrombus formation)					
	BMY 20844 (5)	anagrelide (2)	**11b**	**12b**	**13d**	**29c**
0.3	NT	NT	145 ± 20 (6)[b]	144 ± 17 (7)[b]	97 ± 14 (37)	137 ± 14 (11)[b]
1.0	145 ± 18 (6)[b]	98 ± 11 (37)	74 ± 11 (52)	70 ± 9 (55)	65 ± 10 (58)	74 ± 14 (52)
3.0	81 ± 4 (48)	68 ± 10 (56)	78 ± 14 (50)	65 ± 12 (58)	NT	62 ± 10 (60)
10.0	51 ± 10 (67)	49 ± 8 (68)	NT	NT	NT	NT

[a] Experiments were performed as previously described.[29a,49] The mean thrombus area from 10 trials 2 h after dosing of the test compound was compared with the mean thrombus area from 10 trials performed in the same rabbit to administration of the drug. Predose control mean thrombus area ± SE = 155 ± 2 μM^2. The results shown are an average from experiments conducted in five different rabbits. [b] Not significant.

Table V. Inhibition of Coronary Artery Occlusion in the Anesthetized Dog by cAMP PDE Inhibitors

dose, mg/kg	mean area under flow-time curve, % seconds ± SE[a] (% inhibition of thrombus formation)					
	BMY 20844 (5)	anagrelide (2)	**11b**	**12b**	**13d**	**29c**
0.01	NT	NT	78 ± 13 (18)[b]	89 ± 11 (39)	NT	NT
0.03	NT	72 ± 7 (6)[b]	109 ± 9 (78)	115 ± 17 (90)	115 ± 5 (90)	115 ± 10 (90)
0.1	97 ± 13 (55)	106 ± 11 (73)	120 ± 13 (100)	111 ± 13 (82)	NT	NT
0.3	110 ± 13 (80)	117 ± 8 (94)	NT	NT	>120 (100)	NT
1.0	130 ± 13 (100)	NT	NT	NT	NT	NT

[a] Experiments were performed as previously described.[29a] The mean area under the curve for vehicle-treated animals = 69 ± 9% seconds. the results shown are from experiments conducted in five animals. [b] Not significant.

active platelet aggregation inhibitor, particularly in human PRP. As would be anticipated on the basis of the SAR that has emerged for this structural class, methylation at N-1 (**29b**) diminishes biological activity in both assays.

One final side-chain variant that was explored as part of this study is that found in pentoxifylline (**48**), a hemorheological agent that exhibits antithrombotic activity and is reported to be a weak cAMP PDE inhibitor.[47] The methyl ketone derivative **32** is a potent inhibitor of cAMP PDE but expresses much less impressive platelet inhibitory properties, a circumstance not appreciably altered upon reduction to the corresponding alcohol **33**.

The rat ex vivo platelet aggregometry protocol was used as a means of identifying candidates for further evaluation in animal models of thrombosis. In this assay, anagrelide (**2**) and BMY 20844 (**5**) exhibit IC_{50}'s of 4.9 and 3.2 mg/kg, respectively.[2] However, the marked increase in activity observed in vitro for some of the compounds presented in Table III, when compared to the simpler compounds **2** and **5**, did not translate into enhanced potency in this paradigm. The variation in potency for the series of compounds examined in this model is quite extensive, presumably due to the differing pharmacokinetic properties of the individual agents. The most potent inhibitors of ADP-induced platelet aggregation measured ex vivo using this model are amides **13d**, **13e**, and **13m**, but they do not offer a substantial advantage over some of the more simply substituted compounds studied earlier.[2] The N-1 methylated compound **13e**, although 1 order of magnitude less effective than **13d** in vitro, is comparable in the ex vivo paradigm, demonstrating that reduced intrinsic potency can readily be compensated for by improved pharmacokinetic properties. The ester **11b** and acid **12b** are equipotent and are probably the same agent in vivo based on the propensity with which **11b** is hydrolyzed to **12b** in plasma in vitro.[48] Consistent with this notion, the metabolically more stable isopropyl ester **11d** is much less effective in the ex vivo experiment and the methyl ester **11h** does not show significant activity, presumably because it is efficiently converted to the corresponding inactive acid **12f** during absorption. Interestingly, the ester **13w** potently inhibits ADP-induced platelet aggregation measured ex vivo in the rat, suggesting that enzymatic cleavage to the corresponding acid **13y** is slow in vivo, probably due to steric encumberance by the cyclohexyl substituent.

Two different animal models of thrombosis were employed to evaluate the antithrombotic potential of platelet aggregation inhibitors identified in this study. The biolaser model of small vessel thrombosis, conducted in conscious

(47) Michael, M.; Giessinger, N.; Schroer, R. Reduced Thrombus Formation In Vivo after Administration of Pentoxifylline (Trental). *Thromb. Res.* **1989**, *56*, 359–368.

(48) Russell, J. W. Unpublished observations. The half-life of methyl ester **11b** in human plasma is estimated to be 18 min while that of ethyl ester **11c** is estimated to be 33 min. The isopropyl ester **11d** was not significantly hydrolyzed during a 2-h incubation period.

rabbits, uses a ruby laser to induce thrombus formation in the microvasculature of the ear.[29a,49] Drug candidates are dosed orally 2 h prior to firing of the laser and the mean thrombus area in 10 separate blood vessels is compared with predrug values in the same rabbit. The results are compiled in Table IV along with comparative data for BMY 20844 (5) and anagrelide (2). To evaluate drug effects on large vessel thrombosis, a modified Folts-type paradigm was used.[50,51] In this model, thrombus formation is induced in the left anterior descending coronary artery of anesthetized dogs by the combination of an iron ring placed around the vessel to produce stenosis and application of a small electrical current.[29a] The drug is administered id 45 min before initiating thrombus formation, which is monitored by measuring blood flow distal to the stenosis. The results for compounds evaluated in this model are presented in Table V. It is apparent from an examination of the data presented in Tables IV and V that the compounds identified in this study, **11b**, **12b**, **13d**, and **29c**, are significantly more effective antithrombotic agents in these models than either BMY 20844 (5) or anagrelide (2). This is particularly evident in the modified Folts model of arterial thrombosis where a potent inhibitory effect is seen at doses of **11b**, **12b**, **13d**, and **29c** as low 0.03 mg/kg, representing 1 order of magnitude improvement compared to the activity observed with **5** and **2**.

In attempting to develop candidates for clinical evaluation, we have placed particular emphasis on identifying platelet inhibitors that provide effective antithrombotic activity while incurring minimal hemodynamic burden. Several of the compounds listed in Table III were profiled for their effects on heart rate (HR), mean arterial blood pressure (MABP), and right ventricular contractile force (RVCF) in anesthetized ferrets following id administration. Consistent with inhibition of low-K_m cAMP PDE as a mechanistic basis for inhibition of platelet function, many of these compounds were found to elicit a dose-dependent increase in RVCF and HR which was accompanied by a decrease in MABP. The hemodynamic effects of amide **13d** are particularly pronounced with maximum changes in RVCF, HR, and MABP of +41%, +15%, and −27% at a dose of 0.3 mg/kg id and +35%, +22%, and −30% at a dose of 3 mg/kg, respectively. The effects of sulfone **29c** (BMY 21638)[52] are milder with maximum changes in RVCF, HR, and MABP of +16%, +13%, and −9% at 3 mg/kg and +39%, +31%, and −11% at 10 mg/kg, respectively. However, since both **13d** and **29c** express antithrombotic activity in vivo at doses as low as 0.03 mg/kg, some separation of pharmacological properties may be possible. In the modified Folts model, both **13d** and **29c** caused only minor changes in HR, MABP, and RVCF during the pre-stenosis period at doses providing significant antithrombotic protection.

The unusual properties of ester **11b** (BMY 21259) and the corresponding acid **12b** (BMY 21260) that were detected in the in vitro aggregometry screen were manifest in vivo. These compounds proved to be unique within the imidazo[4,5-*b*]quinolin-2-one series of platelet cAMP PDE inhibitors in that they were hemodynamically silent in the ferret following id administration of doses as high as 10 mg/kg.[53] This profile was confirmed in the dog, thus allowing a direct comparison with the antithrombotic effects observed in the Folts-type model. Administration of a dose of 10 mg/kg id of ester **11b** or acid **12b** to anesthetized dogs caused no significant alteration in RVCF, HR, or MABP, compared to control. (The range of control values were as follows: RVCF, 101 ± 3 to 108 ± 5 g; HR, 161 ± 11 to 169 ± 11 bpm; MABP, 121 ± 2 to 137 ± 2 mmHg. Graphs are presented in the supplementary material.) Thus, cardiovascular parameters were not significantly different from those of the control at a dose over 100-fold higher than that providing complete protection against thrombosis in the Folts-type model. The origin of this remarkable separation in properties in vivo is not clear but would appear not to be based on inhibition of cAMP PDE alone since **11b** and **12b** are effective inhibitors of myocardial cAMP PDE from a variety of species.[53,54] The observed pharmacological profile is presumably the result of a selective action of **11b** and/or **12b** on platelets that may be unrelated to inhibition of platelet cAMP PDE, combined with a limited permeability across the membranes of other cardiovascular tissue. Selective expression of pharmacological activity in vivo by low-K_m cAMP PDE inhibitors does have precedence[55] but of a different nature to that observed for **11b** and **12b**. The imidazolone **49** has been reported to produce a selective positive inotropic effect in vivo with little hypotensive activity.[55]

Conclusion

In summary, the data presented in Table III demonstrates that the potent cAMP PDE and blood platelet inhibitory activity reported for simply substituted imidazo[4,5-*b*]quinolin-2-one derivatives can be enhanced by the introduction of functionalized side chains at C-7 of the heterocyclic nucleus. The structure–activity relationships reported in Table III are consistent with the notion of a secondary binding site proximate to the active site of platelet low-K_m cAMP PDE[25,26] and provide further insight into steric and electronic demands associated with this region. The poor correlation between inhibition of cAMP PDE and platelet aggregation for several representatives of this structural type can be accounted for by variations in membrane permeability, consistent with the hypothesis of an optimum lipophilic window for effective drug delivery.[26,27] Although several of the compounds presented

(49) Fleming, J. S.; Buchanan, J. O.; King, S. P.; Cornish, B. T.; Bierwagen, M. E. Use of the Biolaser in the Evaluation of Antithrombotic Agents. *Platelets and Thrombosis*; Scriabine, A., Sherry, S., Eds.; Baltimore University Park Press: Baltimore, 1974; pp 247–262.

(50) Folts, J. D. Experimental Arterial Platelet Thrombosis, Platelet Inhibitors, and Their Possible Clinical Relevance. *Cardiovasc. Rev. Rep.* **1982**, *3*, 370–382.

(51) Folts, J. D.; Gallagher, K.; Rowe, G. C. Blood Flow Reduction in Stenosed Canine Coronary Arteries: Vasospasm or Platelet Aggregation? *Circulation* **1982**, *65*, 248–255.

(52) Fleming, J. S.; Buchanan, J. O.; Baryla, U. M.; Seiler, S. M.; Meanwell, N. A.; Gillespie, E.; Keely, S. L. BMY 21638, A New, Potent Broad-Spectrum Inhibitor of Blood Platelet Aggregation and Experimental Thrombosis. *Thromb. Haemostasis* **1989**, *62*, 409.

(53) Meanwell, N. A.; Wright, J. J. K.; Fleming, J. S.; Gillespie, E.; Stanton, H. C. BMY 21259 and BMY 21260: Potent Inhibitors of Fraction III Phosphodiesterase, Blood Platelet Aggregation and Experimental Thrombosis that do not Exhibit Cardiotonic or Hypotensive Activity. Xth International Symposium on Medicinal Chemistry, Budapest, Hungary, August 15–19, 1988; P-214.

(54) The ester **11b** half-maximally inhibits purified rabbit heart cAMP PDE III at a concentration of 10^{-6} M while the IC_{50} for acid **12b** is 5×10^{-6} M (Seiler, S. M.; Gillespie, E. Unpublished observations).

(55) Hagedorn, A. A., III; Erhardt, P. W.; Lumma, W. C., Jr.; Wohl, R. A.; Cantor, E.; Chou, Y-L.; Ingebretsen, W. R.; Lampe, J. W.; Pang, D.; Pease, C. A.; Wiggins, J. Cardiotonic Agents. 2. (Imidazolyl)aroylimidazolones, Highly Potent and Selective Positive Inotropic Agents. *J. Med. Chem.* **1987**, *30*, 1342–1347.

in Table III have demonstrated potent antithrombotic activity in animal models, many exhibit the hemodynamic effects expected of low-K_m cAMP PDE inhibitors. However, the ester **11b** and its corresponding acid **12b** present a unique pharmacological profile in that they are hemodynamically silent in dogs at doses 2 orders of magnitude above that required for complete protection in a Folts-type paradigm. Although the biochemical basis for the selective expression of antithrombotic activity by **11b** and **12b** in vivo is not readily apparent, it may be the result of a non-cAMP PDE-based mechanism. Nevertheless, the pharmacological properties of **11b** and **12b** suggest that they would be of clinical value as antithrombotic agents.

Experimental Section

Melting points were recorded on a Thomas-Hoover capillary apparatus and are uncorrected. Magnetic resonance (NMR) spectra were recorded on a Bruker AM FT instrument operating at 300 MHz for proton (^{1}H) and 75 MHz for carbon (^{13}C) or a Perkin-Elmer R32 90-MHz CW spectrometer (^{1}H). All spectra were recorded using tetramethylsilane as an internal standard, and signal multiplicity was designated according to the following abbreviations: s = singlet, d = doublet, t = triplet, q = quartet, m = multiplet, bs = broad singlet. Infrared (IR) spectra were obtained using a Nicolet MX1 FT spectrometer, scanning from 4000 to 400 cm^{-1} and calibrated to the 1601 cm^{-1} absorption of a polystyrene film. Mass spectral data were obtained on a Finnigan Model 4500 GC/MS using chemical ionization (isobutane) procedures. Analytical samples were dried in vacuo at −78 °C or in the presence of P_2O_5 at room temperature for at least 12 h. Elemental analyses were provided by Bristol-Myers Squibb's Analytical Chemistry Department and C, H, and N values are within ±0.4 of calculated values.

Ethyl 4-[3-[(2,4-Dioxoimidazolidin-5-ylidene)methyl]-4-nitrophenoxy]butanoate (9, n = 3, R = Et, R^1 = R^2 = H). Na (4.92 g, 0.21 g-atom) was dissolved in EtOH (600 mL), and diethyl 2,4-dioxoimidazolidine-5-phosphonate (**8a**)[31] (50.5 g, 0.21 mol) was added. After 10 min, a solution of ethyl 4-(3-formyl-4-nitrophenoxy)butanoate[26] (50.0 g, 0.18 mol) in EtOH (100 mL) was added in one portion. The mixture was stirred for 2 h, concentrated to ca. 250 mL in vacuo, diluted with H_2O, and filtered to give **9** (n = 3, R = Et, R^1 = R^2 = H) (61.3 g, 95%) as a 4:1 mixture of *Z*:*E* geometrical isomers. Recrystallization of a sample from EtOH/H_2O gave an analytically pure sample of (*Z*)-**9** (n = 3, R = Et, R^1 = R^2 = H), mp 131–134 °C. Anal. ($C_{16}H_{17}N_3O_7$) C, H, N.

Methyl 4-[(2,3-Dihydro-2-oxo-1*H*-imidazo[4,5-*b*]quinolin-7-yl)oxy]butanoate (11b). A solution of **9** (n = 3, R = Et, R^1 = R^2 = H) (12.75 g, 38 mmol) in DMF (185 mL) was hydrogenated over 10% Pd on C (1.28 g) at 60 psi using a Parr hydrogenation apparatus. After H_2 uptake had ceased, the mixture was filtered through Celite and concentrated in vacuo and MeOH (250 mL) added to the residue. The mixture was heated to reflux, I_2 (9.64 g, 38 mmol) added portionwise, and heating continued for 30 min. The mixture was cooled, concentrated to ca. 25 mL, and diluted with 10% Na_2CO_3 solution until pH = 7 and then 10% $Na_2S_2O_3$ solution was added to precipitate **11b** (8.77 g, 77%). An analytical sample, recrystallized twice from DMF/H_2O, had mp 299–301 °C. Anal. ($C_{15}H_{15}N_3O_4$) C, H, N.

4-[(2,3-Dihydro-2-oxo-1*H*-imidazo[4,5-*b*]quinolin-7-yl)oxy]butyric Acid (12b). A mixture of **11b** (1.00 g, 3.3 mmol), 4 N NaOH solution (2 mL), H_2O (15 mL), and MeOH (15 mL) was stirred at room temperature. After 1 h, 2 N HCl solution was added until pH = 3 and the precipitate filtered, washed sequentially with H_2O, MeOH, and Et_2O, and dried to give **11b** (0.84 g, 88%). Recrystallization from DMF/H_2O gave analytically pure material, mp 327–330 °C. Anal. ($C_{14}H_{13}N_3O_4$) C, H, N.

4-[4-[(2,3-Dihydro-2-oxo-1*H*-imidazo[4,5-*b*]quinolin-7-yl)oxy]-1-oxobutyl]morpholine (13v). DPPA[32] (2.15 g, 1.68 mL, 7.8 mmol) was added to a stirred mixture of **12b** (2.01 g, 7 mmol), morpholine (0.68 g, 7.8 mmol), Et_3N (1.53 g, 2.1 mL, 15 mmol), DMAP (catalytic quantity), and DMF (60 mL). After stirring overnight at room temperature, the mixture was diluted with CH_2Cl_2 (200 mL) and filtered to give **13v** (2.08 g, 84%). An analytical sample was recrystallized from aqueous DMF and had mp 274–276 °C. Anal. ($C_{18}H_{20}N_4O_4$) C, H, N.

3-[(2,3-Dihydro-1*H*-imidazo[4,5-*b*]quinolin-7-yl)oxy]propyl Acetate (16c). A mixture of **6** (47.70 g, 0.285 mol), pulverized K_2CO_3 (43.40 g, 0.314 mol), KI (1.00 g), 3-bromopropyl acetate (56.88 g, 0.314 mol), and DMF (400 mL) was stirred at 110 °C. After 3 h, the mixture was cooled, diluted with H_2O, and extracted with CH_2Cl_2 (4 × 500 mL). The combined extracts were washed with H_2O (4 × 500 mL), dried ($MgSO_4$), and concentrated to leave an oil (77.00 g). This was dissolved in CH_3CN (1 L), phosphonate **8a** (81.70 g, 0.346 mol) was added followed by Et_3N (35.00 g, 48.2 mL, 0.346 mol). The mixture was stirred at room temperature for 1 h, concentrated in vacuo, and diluted with H_2O to give a yellow solid (94.5 g, 95%), used without further purification. An analytical sample was recrystallized from EtOH/H_2O to give a 7.5:1 mixture of (*Z*)- and (*E*)-3-[3-[(2,4-dioxoimidazolidin-5-ylidene)methyl]-4-nitrophenoxy]propyl acetate (**15c**), mp 94–130 °C. Anal. ($C_{15}H_{15}N_3O_7$) C, H, N.

A solution of crude **15c** (83.00 g, 0.238 mol) in DMF (500 mL) was hydrogenated at 400 psi over 10% Pd on C (8.50 g) in a Parr reactor. After H_2 uptake had ceased, the mixture was filtered through Celite and concentrated in vacuo to leave an oil, which was dissolved in CH_3CN (500 mL). *p*-TsOH (1.00 g) was added and the mixture heated at reflux for 1 h before introduction of I_2 (60.4 g, 0.238 mol) portionwise. After 15 min at reflux, the mixture was cooled, diluted with 10% Na_2CO_3 solution (240 mL) and 10% $Na_2S_2O_3$ solution (590 mL), and concentrated. The residue was diluted with H_2O and filtered to give **16c** (64.66 g, 90%). An analytical sample was recrystallized from DMF/H_2O and had mp 301–303 °C. Anal. ($C_{15}H_{15}N_3O_4$) C, H, N.

1,3-Dihydro-7-(3-hydroxypropoxy)-2*H*-imidazo[4,5-*b*]quinolin-2-one (17b). A mixture of **16c** (58.64 g, 0.195 mol), 4 N NaOH solution (145 mL, 0.584 mol), MeOH (175 mL), and H_2O (700 mL) was stirred at room temperature for 2 h. The mixture was acidified with 2 N HCl (300 mL) and filtered to give **17b** (48.73 g, 96%). An analytical sample was recrystallized from DMF/H_2O and had mp 343–345 °C dec. Anal. ($C_{13}H_{13}N_3O_3$) C, H, N.

7-(3-Bromopropoxy)-1,3-dihydro-2*H*-imidazo[4,5-*b*]quinolin-2-one. $SOBr_2$ (8.02 g, 38 mmol) was added dropwise to a stirred suspension of **17b** (5.00 g, 19 mmol) in DMF (75 mL) maintained at 0 °C. After 2 h, the mixture was diluted with H_2O, 10% Na_2CO_3 solution added until pH = 8, and the mixture filtered to give the title compound (5.73 g, 92%). An analytical sample was recrystallized from DMF/MeOH and had mp 246–250 °C. Anal. ($C_{13}H_{12}BrN_3O_2$) C, H, N.

7-[(3-Cyanopropyl)oxy]-2,3-dihydro-2-oxo-1*H*-imidazo[4,5-*b*]quinoline-1,3-diyldimethyl Bis(2,2-dimethylpropanoate) (22a). A mixture of 7-(3-bromopropoxy)-1,3-dihydro-2*H*-imidazo[4,5-*b*]quinolin-2-one (5.00 g, 15.5 mmol), NaCN (2.28 g, 46.5 mmol), H_2O (15 mL), and DMF (50 mL) was stirred at room temperature for 30 min and 70 °C for 18 h before being cooled and diluted with H_2O (150 mL). Filtration gave a white solid (2.78 g, 66%, 10.4 mmol) which was mixed with (pivaloyloxy)methyl chloride (4.00 g, 26 mmol), K_2CO_3 (2.87 g, 21 mmol), and DMF (50 mL) and stirred at 110 °C. After 45 min, the mixture was cooled, diluted with H_2O (75 mL), and extracted with Et_2O (4 × 100 mL). The combined extracts were washed with H_2O (3 × 150 mL), dried over $MgSO_4$, and concentrated to leave an oil. Chromatography on silica gel using a mixture of hexanes and EtOAc (7:3) as eluant gave **22a** (2.00 g, 39%). An analytical sample was prepared by recrystallization from hexanes/EtOAc and had mp 131–133 °C. Anal. ($C_{28}H_{32}N_4O_6$) C, H, N.

7-[(3-Cyanopropyl)oxy]-1,3-dihydro-2*H*-imidazo[4,5-*b*]quinolin-2-one (21a). A mixture of **22a** (3.80 g, 7.7 mmol), 5 N KOH (3.32 mL, 16 mmol), and MeOH (25 mL) was stirred at room temperature for 45 min. Concentrated H_2SO_4 was added until pH = 3 and the mixture stirred at reflux for 4 h, room temperature for 18 h, reflux for 7 h, and room temperature for 18 h. The solvent was evaporated, and the residue was diluted with H_2O and filtered to give a solid, which was dissolved in hot DMF. Addition of MeOH gave **21a** (1.44 g, 70%), mp 328–332 °C dec. Anal. ($C_{14}H_{12}N_4O_2 \cdot 0.1CH_3OH$) C, H, N.

1,3-Dihydro-7-[3-(2*H*-tetrazol-5-yl)propoxy]-2*H*-imidazo[4,5-*b*]quinolin-2-one (23a). A mixture of **22a** (5.40 g, 11 mmol), nBu_3SnN_3[34] (5.40 g, 16 mmol), and toluene (25 mL) was stirred at 105 °C for 65 h. The mixture was cooled and 10% HCl in EtOH solution (3.5 mL) was added followed by MeOH (100 mL). The

mixture was concentrated to leave a waxy solid which was triturated with Et_2O to give a white solid (4.98 g, 85%). This was combined with 5 N NaOH solution (9.2 mL, 46 mmol) and MeOH (100 mL) and stirred overnight at room temperature. The solvent was evaporated and the residue suspended in a mixture of H_2O (85 mL) and DMF (1 mL) and concentrated H_2SO_4 (70 drops) added. The mixture was heated at reflux for 6 h, cooled, stirred at room temperature for 65 h, and filtered. The solid was dissolved in hot DMF (18 mL) and diluted with H_2O to give **23a** (1.67 g, 62%), mp 295–324 °C dec. Anal. ($C_{14}H_{13}N_7O_2$·0.07DMF) C, H, N.

7-[4-(1-Cyclohexyl-1*H*-tetrazol-5-yl)butoxy]-1,3-dihydro-2*H*-imidazo[4,5-*b*]quinolin-2-one Hydrochloride (25). Na (1.38 g, 0.06 g-atom) was dissolved in EtOH (250 mL) and phosphonate **8a** (14.22 g, 60 mmol) added. After 5 min, aldehyde **24**[25b] (17.30 g, 46 mmol) in EtOH (50 mL) and CH_2Cl_2 (50 mL) was added in one portion and the mixture stirred for 10 min. The solvent was evaporated, the residue diluted with H_2O and 2 N HCl, and a yellow solid filtered off and dried in air to give the benzylidene hydantoin derivative (18.38 g, 87%). A sample was recrystallized from DMF/H_2O to give analytically pure material, melting point indistinct, as a 3:1 mixture of *Z*:*E* isomers. Anal. ($C_{21}H_{25}N_7O_5$·0.2H_2O) C, H, N, H_2O.

A solution of this material (12.00 g, 26 mmol) in DMF (200 mL) was hydrogenated over 10% Pd on C at 55 psi in a Parr hydrogenation apparatus. After H_2 uptake had ceased, the mixture was filtered through Celite and the solvent removed. The residue was suspended in MeOH at reflux, I_2 (6.69 g, 26 mmol) added portionwise over 4 min, and the mixture heated at reflux for 10 min. The mixture was concentrated in vacuo to ca. 70 mL, diluted with 10% Na_2CO_3 solution and 10% $Na_2S_2O_3$ solution, and filtered. The solid was dissolved in hot DMF, precipitated with H_2O, and then dissolved in a 10% solution of dry HCl in MeOH. Removal of the MeOH and recrystallization of the residue from EtOH afforded **25** (2.16 g, 18%), mp 288–291 °C. Anal. ($C_{21}H_{25}N_7O_2$·HCl) C, H, N.

7-[4-(Phenylsulfonyl)butoxy]-1,3-dihydro-2*H*-imidazo[4,5-*b*]quinolin-2-one (29c). A mixture of [4-(chlorobutyl)sulfonyl]benzene (**26**, *n* = 4) (5.00 g, 21 mmol), **6** (3.34 g, 20 mmol), K_2CO_3 (3.00 g, 22 mmol), KI (catalytic quantity), and DMF (75 mL) was heated at reflux for 4 h. The mixture was cooled, diluted with H_2O, and extracted with Et_2O. The combined extracts were washed with H_2O, dried over Na_2SO_4, and concentrated to give **27** (*n* = 4) (4.70 g, 69%).

Na (0.386 g, 0.017 g-atom) was dissolved in EtOH (70 mL) and **8a** (3.96 g, 17 mmol) added. After stirring for 1 h, a solution of **27** (*n* = 4) (4.70 g, 13 mmol) in a mixture of EtOH and $CHCl_3$ was added and the mixture stirred for 20 min before being concentrated, diluted with H_2O, and extracted with $CHCl_3$ to give a foam (4.60 g, 61%). An analytical sample, recrystallized from CH_3CN/Et_2O, had mp 150–152 °C and was pure *Z* isomer. Anal. ($C_{20}H_{19}N_3O_7S$) C, H, N.

A solution of the crude material (4.12 g, 9.2 mmol) in DMF (125 mL) was hydrogenated over 10% Pd on C at 60 psi in a Parr hydrogenation apparatus. After H_2 uptake had ceased, the mixture was filtered through Celite, the solvent evaporated, and the residue dissolved in MeOH at reflux. I_2 (2.35 g, 9 mmol) was added and the mixture heated at reflux for 1 h and cooled. A 10% solution of Na_2CO_3 was added followed by 10% $Na_2S_2O_3$ solution. The precipitated solid was collected and recrystallized from DMF/H_2O/CH_3CN to give **29c** (1.90 g, 51%), mp 258 °C dec. Anal. ($C_{20}H_{19}N_3O_4S$·0.2H_2O) C, H, N, H_2O.

1,3-Dihydro-7-(4-oxopentoxy)-2*H*-imidazo[4,5-*b*]quinolin-2-one (32). A solution of 5-[[5-[3-(2-methyl-1,3-dioxolan-2-yl)propoxy]-2-nitrophenyl]methylene]-2,4-imidazolidinedione (34.7 g, 92 mmol) in DMF (500 mL) was hydrogenated over 10% Pd on C (3.5 g) at 200 psi in a Parr reactor vessel. After 18 h, the mixture was filtered through Celite and concentrated in vacuo to afford a beige solid. This was suspended in MeOH (500 mL) at reflux, I_2 (23.3 g, 92 mmol) added portionwise, and the mixture heated at reflux for 30 min. The mixture was cooled, diluted with H_2O (200 mL), and stirred for 15 min. A 10% solution of Na_2CO_3 (75 mL) and a 10% $Na_2S_2O_3$ solution (230 mL) were added, and the mixture was concentrated to ca. 600 mL. The precipitate was filtered off and dried in vacuo at 70 °C to give **32** (22.10 g, 84%). An analytical sample was prepared by recrystallization from DMF/H_2O and had mp 294–296 °C dec. Anal. ($C_{15}H_{15}N_3O_3$) C, H, N.

1,3-Dihydro-7-(4-hydroxypentoxy)-2*H*-imidazo[4,5-*b*]quinolin-2-one (33). $NaBH_4$ (1.00 g, 26 mmol) was added portionwise to a stirred suspension of **32** (3.70 g, 13 mmol) in MeOH (85 mL) and DMF (85 mL). After stirring at room temperature for 3 h, the solvent was evaporated and the residue triturated with H_2O (50 mL). A solid was filtered off, recrystallized from DMF/H_2O, and triturated with MeOH to give **33** (3.20 g, 86%), mp 301–303 °C. Anal. ($C_{15}H_{17}N_3O_3$) C, H, N.

***N*-[2-[(2,4-Dioxo-5-imidazolidinyl)methyl]phenyl]acetamide.** A solution of **35**[31] (47.00 g, 0.19 mol) in DMF (400 mL) was hydrogenated over 10% Pd on C (3.00 g) at 50 psi in a Parr hydrogenation apparatus. After 7 h, the mixture was filtered through Celite, the solvent evaporated, and the residue triturated with H_2O. After standing overnight at 5 °C, the solid was collected, washed with H_2O, and dried in vacuo at 80 °C to give the title compound (47.15 g, 100%). An analytical sample was purified by recrystallization from EtOH/H_2O and had mp 200–202 °C. Anal. ($C_{12}H_{13}N_3O_3$·0.1H_2O) C, H, N.

***N*-[4-Bromo-2-[(2,4-dioxo-5-imidazolidinyl)methyl]phenyl]acetamide (36).** Bromine (23.26 g, 0.146 mol) in AcOH (10 mL) was added dropwise to a stirred solution of *N*-[2-[(2,4-dioxoimidazolidinyl)methyl]phenyl]acetamide (34.24 g, 0.139 mol) and NaOAc (12.54 g, 0.153 mol) in AcOH (300 mL) maintained at 65 °C. The mixture was stirred at 65 °C for 18 h, cooled, diluted with H_2O (1 L) and 10% Na_2SO_3 solution, and filtered to give a white solid (17.00 g). The filtrate was concentrated to give a white solid which was triturated in H_2O and filtered to give an additional 17.00 g of product. The combined solids were washed with Et_2O and dried in vacuo to give **36** (30.78 g, 94%). An analytical sample was obtained by recrystallization from EtOH and had mp 216–220 °C. Anal. ($C_{12}H_{12}BrN_3O_3$) C, H, N.

7-Bromo-1,3-dihydro-2*H*-imidazo[4,5-*b*]quinolin-2-one (37). A mixture of **36** (30.78 g, 94 mmol), EtOH (375 mL), and 10% HCl solution (190 mL) was heated at reflux for 2.5 h. The mixture was cooled to 5 °C and filtered to give a solid (18.58 g). The filtrate was concentrated in vacuo and neutralized with $NaHCO_3$, and the solid was filtered and heated with EtOH (15 mL) and 10% HCl solution (10 mL) for 1.5 h. The mixture was cooled and filtered and the solid combined with the previously isolated material to give 5-[(2-amino-5-bromophenyl)methyl]-2,4-imidazolidinedione (20.53 g, 77%), mp >310 °C. Anal. ($C_{10}H_{10}BrN_3O_2$) C, H, N.

I_2 (8.93 g, 0.35 mmol) was added in one portion to a solution of 5-[(2-amino-5-bromophenyl)methyl]-2,4-imidazolidinedione (10.00 g, 35 mmol) in DMF (150 mL) maintained at reflux. After 5 min, the mixture was cooled to room temperature, diluted with H_2O, and Na_2SO_3 solution added until colorless. Na_2CO_3 solution (10%) was added until pH = 9, and the solid was filtered off, washed with H_2O and EtOH, and dried to give **37** (8.45 g, 90%), mp >310 °C. Anal. ($C_{10}H_6BrN_3O$) C, H, N.

7-Bromo-1,3-bis[dimethyl(1,1-dimethylethyl)silyl]-2*H*-imidazo[4,5-*b*]quinolin-2-one (38). NaH (8.36 g of a 50% dispersion in mineral oil, 174 mmol) was washed several times with pentane, and covered with anhydrous THF (400 mL) and **37** (20.00 g, 76 mmol) added. *tert*-Butyldimethylsilyl chloride (25.14 g, 167 mmol) was added in one portion, and the mixture was stirred at room temperature for 15 min and then at reflux. After 30 min, additional *tert*-butyldimethylsilyl chloride (2.28 g, 15 mmol) was added and the mixture heated at reflux for 20 min before being stirred at room temperature for 1 h. The mixture was filtered through Celite and concentrated in vacuo and the residue triturated with pentane to afford a white powder, which was recrystallized from hexanes to give **38** (30.69 g, 82%), mp 176–178 °C. Anal. ($C_{22}H_{34}BrN_3OSi_2$) C, H, N.

Methyl 5-(2,3-Dihydro-2-oxo-1*H*-imidazo[4,5-*b*]quinolin-7-yl)-2,4-pentadienoate (40b). A mixture of **38** (5.00 g, 10.2 mmol), methyl 1,3-butadiene-1-carboxylate[38] (1.42 g, 12.7 mmol), $Pd(OAc)_2$ (69 mg, 0.3 mmol), tri-*o*-tolylphosphine (464 mg, 1.5 mmol), Et_3N (3 mL), and CH_3CN (3 mL) was placed in a heavy-walled sealed glass tube. The mixture was warmed in a water bath at 75 °C until solution occurred and then placed in an oil bath maintained at 100 °C. After 20 h, the mixture was cooled, filtered, and concentrated in vacuo. The residue was purified by chromatography on a column of silica gel[56] using a

mixture of hexanes and Et_2O (gradient of 18:1, 16:1, 14:1 and then 10:1) to give **39b** (3.52 g, 66%). An analytical sample was prepared by recrystallization from EtOAc/hexanes and had mp 158–160 °C. Anal. ($C_{28}H_{41}N_3O_3Si_2$) C, H, N.

A solution of **39b** (500 mg, 0.96 mmol) in MeOH (15 mL) containing a catalytic quantity of *p*-TsOH was heated at reflux. After 30 min, the mixture was poured onto H_2O, Na_2CO_3 added until pH = 7–8 and filtered to give **40b** (288 mg, 100%), mp >310 °C. Anal. ($C_{18}H_{13}N_3O_3 \cdot 0.1H_2O$) C, H, N.

Methyl 5-(2,3-Dihydro-2-oxo-1*H*-imidazo[4,5-*b*]quinolin-7-yl)pentanoate (41b). A solution of **39b** (1.00 g, 2 mmol) in EtOAc (10 mL) was hydrogenated over 10% Pd on C (50 mg) at 50 psi in a Parr hydrogenation apparatus. After H_2 uptake had ceased, the mixture was filtered through Celite and concentrated and the residue dissolved in MeOH (20 mL) containing a catalytic amount of *p*-TsOH. The mixture was heated at reflux for 30 min, cooled, diluted with water, and filtered to give **41b** (513 mg, 90%), mp 293–295 °C. Anal. ($C_{18}H_{17}N_3O_3$) C, H, N.

5-(2,3-Dihydro-2-oxo-1*H*-imidazo[4,5-*b*]quinolin-7-yl)-pentanoic Acid (42). A mixture of **41b** (832 mg, 1.5 mmol), 1 N KOH solution (10 mL), and MeOH (4 mL) was stirred at room temperature for 18 h. The mixture was diluted with 10% HCl solution (10 mL), heated at reflux for 30 min, and then cooled and Na_2CO_3 added until pH = 5. Filtration gave **42** (333 mg, 74%), mp >310 °C. Anal. ($C_{15}H_{15}N_3O_3$) C, H, N.

***N*-Cyclohexyl-2,3-dihydro-2-oxo-1*H*-imidazo[4,5-*b*]-quinoline-7-pentanamide (43b).** A mixture of **42** (670 mg, 2.3 mmol), cyclohexylamine (0.35 g, 0.4 mL, 3.5 mmol), Et_3N (0.47 g, 0.64 mL, 4.6 mmol), DPPA[32] (0.71 g, 0.55 mL, 2.5 mmol), and DMF (30 mL) was stirred at room temperature for 18 h. The mixture was diluted with H_2O, the solvent evaporated, and the residual solid triturated with MeOH and filtered to give **43b**. Recrystallization from DMF/H_2O gave analytically pure **43b** (580 mg, 68%), mp >315 °C. Anal. ($C_{21}H_{26}N_4O_2 \cdot 0.1DMF$) C, H, N.

1,3-Dihydro-7-(5-hydroxypentyl)-2*H*-imidazo[4,5-*b*]-quinolin-2-one (44b). A solution of **39b** (1.10 g, 2.1 mmol) in EtOAc (10 mL) was hydrogenated over 10% Pd on C (50 mg) at 50 psi in a Parr hydrogenation apparatus. After H_2 uptake had ceased, the mixture was filtered through Celite and concentrated, the residue dissolved in dry THF (8 mL), and $LiAlH_4$ (45 mg, 1 mmol) added portionwise with cooling. After 30 min, an additional 8 mg of $LiAlH_4$ was added, the mixture stirred 30 min, and a saturated solution of Na_2SO_4 added carefully. The mixture was filtered and concentrated and the residue purified by chromatography on silica gel to give the alcohol as a colorless foam (738 mg, 71%). This was dissolved in MeOH (10 mL) containing a catalytic amount of *p*-TsOH, heated at reflux for 30 min, cooled, and diluted with H_2O. Filtration gave **44b** as a white powder (397 mg, 86%), mp >310 °C. Anal. ($C_{15}H_{17}N_3O_2$) C, H, N.

Biological Evaluation. Drug effects on human platelet cAMP and cGMP phosphodiesterase were determined as previously described.[2,24b] Blood platelet aggregometry studies, using rabbit and human PRP, were performed as previously described.[2,39] Ex vivo aggregometry studies following oral administration of test compound to rats was carried out according to the established protocol.[2]

The biolaser model of in vivo thrombosis has been described in detail.[29,39,48] Each rabbit served as its own control and predrug values of mean thrombus area (μM^2) were determined in 10 separate blood vessels following discharge of the laser. Test compound was administered orally as a suspension in H_2O and Tween 20 and the experiment repeated 2 h later. Drug effects were determined by comparing pre- and postdose mean thrombus areas. The results presented in Table IV are an average of experiments conducted in at least three rabbits. Antithrombotic activity in a modified Folts-type model of large vessel thrombosis was determined according to the described protocol, and the results compiled in Table V are an average from at least three individual experiments.[29]

Hemodynamic effects of drug candidates were evaluated in anesthetized ferrets as previously described[29] and the results presented are an average from at least three separate experiments. Hemodynamic effects of **11b** and **12b** were also determined in anesthetized adult beagle dogs of either sex. Anesthesia was induced by iv administration of sodium pentobarbital (30–35 mg/kg) and was maintained by constant infusion of 5 mg/kg per h. A tracheotomy was performed, and the dogs were mechanically respired with a Harvard respirator. The animals were bilaterally vagotomized. The heart was exposed via a midline thoracotomy and a flow probe placed around the ascending arch of the aorta to record aortic blood flow. Right ventricular contractile force (RVCF) was measured with a Walton-Brodie strain gauge arch sutured onto the surface of the ventricle. Mean arterial blood pressure (MABP) was recorded from a saline-filled femoral arterial catheter connected to a Statham pressure transducer. Heart rate was obtained from the pulse pressure signal and recorded with either a cardiotachometer or by direct count of the pulse pressure wave. Catheters were inserted into the brachial or femoral veins for infusion of anesthetic and into the duodenum, exposed by laparotomy, for administration of the test compound. Test drugs were dissolved in DMF and diluted with PEG 400 to give a suspension in 40% DMF/60% PEG 400. Drug volumes ranged from 0.3 to 1.0 mL/kg. In control experiments, animals were administered vehicle (40% DMF/60% PEG 400) in a volume equivalent to 1.0 mL/kg. The results presented in Figure 3 are an average from three separate experiments.

Acknowledgment. We thank C. M. Combs and R. D. Rutkowski for providing and interpreting NMR spectral data, J. G. Schmidt for mass spectral data, and C. L. Kennedy for combustion analyses. A. E. Bosza is acknowledged for her help in preparing the manuscript.

Supplementary Material Available: Spectroscopic and analytical data for imidazo[4,5-*b*]quinolin-2-one derivatives and intermediates prepared for this study and graphs of the effects of 0.1 mg/kg id of **11b** and 0.03 mg/kg of **29c** in the coronary stenosis–occlusion model, and graphs of the effects of **11b** and **12b** on hemodynamic parameters in anesthetized dogs following id administration of a dose of 10 mg/kg (12 pages). Ordering information is given on any current masthead page.

(56) Still, W. C.; Kahn, M.; Mitra, A. Rapid Chromatographic Technique for Preparative Separations with Moderate Resolution. *J. Org. Chem.* 1978, *43*, 2923–2925.